ENET 9656360

Bundesamt für Energie
Office fédéral de l'énergie
Ufficio federale dell'energia
Swiss Federal Office of Energy

Programme
Active solar energy, photovoltaics

New generation of Hybrid Solar PV/T collectors

prepared by
LESO-PB / EPFL, Lausanne
Enecolo AG, Mönchaltorf
Ernst Schweizer AG, Hedingen

ÉCOLE POLYTECHNIQUE FÉDÉRALE DE LAUSANNE

LESO-PB / EPFL

Enecolo AG

Ernst Schweizer AG

on behalf of
Swiss Federal Office of Energy

June 2000

Final Report DIS 56360 / 16868

TABLE OF CONTENTS

SUMMARY

Although the idea of a solar collector for both electricity and hot water is not new, the new generation studied here is based on a very innovative concept. During the previous feasibility study we collected comprehensive information about all important aspects (costs, technology, market, contacts with industries, ...) to prove that further development is worth being done. The results were encouraging since they showed:

- A potential market does exist for several specific applications (about 10 MW in 2005)
- The photovoltaic (PV) thin film technology is likely to be suited for this application from a technical and a financial point of view, provided that the long term stability of the cells at temperatures above 100°C is confirmed.
- Several photovoltaic industries are ready to collaborate in this development at different levels of participation.
- The several technical concepts proposed are suited for the concerned application.

World-wide (USA, IEA, ...) there are several projects with the same topic, although with a different working plan (absorption, temperature behaviour and emissivity are not addressed in priority).

The feasibility study showed that the competitiveness of a hybrid collector depends on several technical requirements of the integrated PV-module. The most prominent aspects are high solar absorption, compatibility with high temperatures and a low emissivity.

The goal of the present study is to verify whether these technical conditions are met for the available amorphous silicon (a-Si) technology. Commercial unencapsulated samples from 6 different manufacturers based on different substrates (glass, stainless steel, polyimide) were measured.

Absorption values were measured between 78% and 90%. Two mesurement methods were used (spectrometry, microcalorimetry). Both methods gave close results. A link between the figures found and the three substrate categories could not be established.

Thanks to the thermal cycling test, very valuable data (also for other applications) was gained. Some samples that were stored at 210°C for 10 hours kept their original properties. The other samples showed modified characteristics after this treatment. The stability under thermal cycling seems to be connected to absence of aluminium in the back contacts (Al diffusion). An improved stability can be obtained with a layer of oxide between the back contact and the a-Si films.

Further, the emmissivity coefficients of the samples were measured. The results show that conventional top cover materials like glass, EVA or Tefzel are non-selective materials that have a high emissivity coefficient (between 86 and 95%).

Since the a-Si cells seem to be stable under thermal cycling, our recommendation is to develop a new encapsulating material with a low-e surface and an improved durability under high temperatures, which will enable the construction of a hybrid PV/T collector with the thermal performance of a standard flat plate collector.

ZUSAMMENFASSUNG

Das Konzept einer Kombination von einem Photovoltaik-Generator und einem thermischen Kollektor in einem Gehäuse ist seit mehreren Jahren bekannt. Das vorliegende Projekt untersucht das Konzept mit neuen innovativen Ansätzen. In der Vorstudie wurden verschiedene Informationen evaluiert und zusammengefasst. Aspekte wie Kosten, Technologie, Markt, Kontakte mit der Industrie, usw. wurden untersucht, um aufzuzeigen, dass weitere Entwicklung in diesem Gebiet notwendig ist.

Gemäss der Vorstudie resultierten folgende vielversprechende Resultate:

- Ein potentieller Markt existiert für verschiedene untersuchte Anwendungsbereiche (total ca. 10 MW / Jahr im 2005).
- Die Dünnfilmtechnologie (speziell amorphes Silizium) kann aus technischer und wirtschaftlicher Sicht für unsere Anwendung gut eingesetzt werden, positive Resultate aus Versuchen betreffend Langzeitstabilität von a-Si über 100°C vorbehalten.
- Verschiedene PV- Hersteller sind bereit, sich in diesem Projekt mit unterschiedlichem Engagement an der Mitarbeit zu beteiligen.
- Die technischen Voraussetzungen und Möglichkeiten sprechen für eine Kombination von PV und einem thermischen Kollektor.

Weltweit beschäftigen sich verschiedene Projekte mit diesem Thema (PV/T), wenn auch unter anderen Voraussetzungen und zu untersuchenden Punkten (Absorption, thermisches Verhalten und Emissivität haben unterschiedliche Prioritäten).

Die Vorstudie zeigte klar, dass eine mögliche Markteinführung von verschiedenen technischen Anforderungen für das einzusetzende PV- Modul abhängig ist. Die wichtigsten technischen Anforderungen für die Photovoltaik sind ein hoher Absorptionskoeffizient, gute Temperaturbeständigkeit und eine geringe Emissivität.

Das Ziel dieser Projektphase war die Verifizierung der technischen Anforderungen. Konnten die geforderten Werte für kommerziell erhältliches a- Si eingehalten werden.

Verschiedenes Halbmaterial (nicht laminiert) konnte von 6 Produzenten organisiert werden. Alle Muster auf unterschiedlichen Substraten, wie Glas, rostfreier Stahl und Polyimid wurden betreffend Absorption gemessen. Werte im Bereiche von 78% bis 90% sind gemessen worden. Es wurden zwei unterschiedliche Messmethoden angewandt, eine spektroskopische und eine mikrokaloriemetrische. Für beide Messmethoden resultierten sehr übereinstimmende Werte, die die gemessenen Werte bestätigen. Alle Werte wurden in der jeweiligen Substratkategorie untereinander verglichen.

Weiter wurde mit den Mustern das thermische Verhalten untersucht. Wertvolle Informationen konnten gesammelt werden, dies nicht nur für die einen PV/T- Kollektor sondern evtl. für zusätzliche oder bekannte Anwendungen. Einige Muster zeigten auch nach einem thermischen Dauertest von 10h bei 210°C immer noch ihr Originalverhalten. Andere Muster veränderten sich unter dieser Belastung mehr oder weniger. Die Stabilität eines Produktes wird in Zusammenhang mit einem Fehlen einer

Aluminiumschicht als Rückkontakt gebracht (Al-Diffusion). Eine Verbesserung kann durch eine Oxidschicht zwischen dem Rückkontakt und der a- Si Schicht erzielt werden.

Neben den beiden erwähnten Punkten wurde auch die Emissivität einer a- Si Zelle untersucht. Es resultierte, dass konventionelles Oberflächenmaterial wie Glas, EVA oder TEFZEL sogenannte nicht-selektive Materialien sind. Dies führt zu einem hohen Emissivitätskoeffizient im Bereich von 86% - 95%.

Aus den Untersuchungen folgert die Empfehlung ein neues Verkapselungsmaterial zu entwickeln mit einem sehr niedrigen Emissivitätsfaktor auf der Oberfläche. Zusätzlich sollte die Beständigkeit gegenüber den höheren Temperaturen mittels dem Laminiermaterial verbessert werden. Dies würde zu einem thermischen Verhalten ($Wirkungsgrad_{Thermisch}$) eines PV/T- Kollektors führen, ähnlich wie bei einem normalen Flachkollektor.

RÉSUMÉ

Bien que l'idée de développer un capteur solaire produisant simultanément électricité et eau chaude est connue, la nouvelle génération présentée ici est basée sur un concept tout à fait novateur.

Au cours de l'étude de faisabilité, quantité d'information concernant tous les aspects importants a été collectée (aspects financiers, technologiques, marché, contacts avec l'industrie,...). Les résultats obtenus étaient encourageants puisqu'ils ont montré que :

- Un marché potentiel existe pour les différentes applications proposées.
- La technologie au silicium amorphe convient parfaitement à cette application si la stabilité à long terme pour un fonctionnement au-dessus de 100°C est confirmée.
- Plusieurs industries du photovoltaïque sont prêtes à collaborer à ce développement.

Au plan mondial, plusieurs équipes travaillent sur ce sujet (USA, AIE,...). Leur approche est toutefois fort différente (l'optimisation du coefficient d'absorption et les contraintes thermiques ne représentent pas une priorité dans leurs cas).
L'étude de faisabilité a montré que la compétitivité du capteur hybride dépend de plusieurs critères techniques. Une absorption élevée, un comportement fiable à haute température et une basse émissivité en sont les principaux.
Le but de la présente étude est de vérifier si ces trois critères techniques sont réunis dans le cas des principales technologies silicium amorphe (a-Si). Des échantillons commerciaux provenant de 6 fabricants différents et basés sur différents types de substrats (verre, acier, plastique) ont été testés.

Des valeurs d'absorption entre 78% et 90% ont été mesurées au moyen de deux méthodes complètement différentes (mesures par spectrométrie et par microcalorimétrie). Les résultats obtenus par les deux méthodes sont proches. Les valeurs ne dépendent pas du type de substrat. Pour connaître le comportement des modules amorphes à haute température, une série de cycles thermiques a été effectuée. Certains des échantillons ont conservé leur caractéristiques initiales après avoir été maintenus à 210°C pendant 10 heures. D'autres ont été détruits par ce traitement. Un groupe ad hoc d'experts a été constitué afin d'évaluer ces résultats. Il en ressort que le principal processus de dégradation soit la diffusion d'aluminium présent dans la métallisation arrière. La présence d'oxyde entre le contact arrière et les couches minces de silicium améliore grandement la stabilité en agissant comme barrière antidiffusion. Finalement, l'émissivité des échantillons et de quelques autres types de capteurs photovoltaïques a été mesurée. Les résultats montrent que les matériaux conventionnels tels que le verre, le Tefzel ou l'EVA sont non sélectifs. Leur émissivité est comprise entre 86 et 95%.

Comme les échantillons au silicium amorphe semblent être stable aux hautes températures, notre recommandation est de développer des nouveaux types d'encapsulation avec une surface à basse émissivité et une bonne durabilité à haute température. Ceci permettra au capteur hybride d'offrir des performances proches de celles d'un capteur thermique conventionnel et améliorera grandement sa compétitivité.

1. INTRODUCTION

In the previous feasibility study [1], a-Si was presented as an excellent photovoltaic technology for hybrid application (PV/T). Some requirements needed to be assessed since they were not directly available in the literature. The goal of this Phase 2 was to verify:

- whether the absorption of a-Si modules is sufficient for an acceptable thermal efficiency in domestic hot water applications;
- whether the technology can afford the stagnation situation that will usually occur during regular operation of the solar system.
- what the emissivity coefficients of conventional front surfaces of a-Si modules are.

2. SELECTION OF TEST SAMPLES

In order to select the most appropriate technology for the intended product development, it was decided to perform the tests on commercial a-Si modules. The contact with manufacturers was also an opportunity to get in touch with them for presenting the project and evaluate their interest in participating. Priority was given to European manufacturers, contacts were made in order to propose the following process:

- The manufacturer provides samples to the project team for testing (absorption, thermal cycling)
- Absorption measurements and thermal cycling are done
- Depending on the conditions of the sample delivery of manufacturers (price, information concerning the samples, interest in participating), the measurements were communicated back to the manufacturer.

Decision was taken not to mention company names for the confidentiality of the results (the scientific results are nevertheless available). The samples were requested as non-encapsulated so that the results would concern the cell technology only. Based on these results, then the establishment of a term of reference for the encapsulation is possible.

More than 10 manufacturers were contacted. Only 6 of them accepted to send sample modules. They are from France, Great Britain, Germany and USA. No echo was obtained from Japanese companies. The sample modules are based on substrates made of glass, polyimide and stainless steel. Table 2.1 summarises the tested sample modules.

Sample code	Manu-facturer code	Substrate	Junction type	Encap-sulation	Size			Number of cells	Measurements done	
					Length cm	Width cm	Area cm2		Absorption meas.	Thermal cycling
A	1	glass	single	none	30.5	30.5	930	28	x	x
B	2	glass	tandem	resin	33	15	495	14	x	x
C	3	glass	single	none	11	10.9	120	7	x	x
D	4	glass	single	resin	10	5	50	5	x	x
E	3	glass	single	resin	11	10.9	120	7	x	
F	5	polyimide	tandem	none	3	3.6	10.8	3	x	
G	6	stainless steel	tandem	none	15.5	4.4	68	1	x	
H	6	stainless steel	triple	EVA / EVA	34.2	23.3	797	1	x	
I	5	polyimide	tandem	EVA / EVA	6	3.6	21.6	6	x	x
J	5	polyimide	tandem	none	24	3.6	86.4	12		x
K	6	stainless steel	triple	none	34.2	23.3	797	1	x	x

Table 2.1: Sample modules available for the tests

3. ABSORPTION ASSESSMENTS

3.1. Introduction

The feasibility study showed that absorption coefficients of standard PV modules should be higher than 80% to make the hybrid PV/T collector financially competitive.

Few data are available from PV manufacturers concerning solar absorption; basic investigations during the feasibility study returned a ~65 % absorption for a commercial module. 1996 Ernst Schweizer AG measured a solar absorption coefficient of ~72 % on a commercial Tefzel-EVA-amorphous module. The "Institut de Microtechnique" in Neuchâtel did more precise measurements in 1996 [2] with a "Perkin Elmer" spectrometer. Coefficients ranging form 78% (a-Si, one layer) to 90% (c-Si) have been measured on special manufactured samples and also on commercial modules.

3.2. Goal

Goal of the present study is to determine the optical absorption of various types of solar cells over the entire range of the solar spectrum.

A series of measurements (spectroscopic and microcalorimetric) was performed in order to show the effective reflections of the different optical layers of photovoltaic devices. This has to be done over the whole solar spectrum. Photovoltaic specialists rarely did it since they were less interested in the wavelengths that do not contribute to the photovoltaic conversion. However, these wavelengths are preferably reflected since they contribute to heating up the photovoltaic device, which decreases electrical efficiency. These measurements were done on 7 available photovoltaic raw material plates of standard devices (glass-substrate, steel and polyimide) and on some laminated samples produced in the framework of this project for comparison.

Two different measuring methods were used to offer a better understanding of the sample properties. The first is based on spectrometry and yields a wavelength-resolution. This was subcontracted to the IMT (Institut de Microtechnique) in Neuchâtel. The second one is based on calorimetry (yields a global value) and was subcontracted to the IOA (Institut d'Optique Appliquée, Département de Microtechnique, EPFL) in Lausanne. The comparison of these results gives a good idea of what kind of data we have to expect for the follow-up of the project and will help us to build a prototype later.

Detailed values of the absorption coefficients of various module types are given. This completes the feasibility study and confirm the competitiveness of the hybrid collector.

3.3. Spectrometric measurements

IMT used a Perkin Elmer UV/VIS/NIR spectrometer (type Lambda 900) to measure the reflection of various samples of solar cells. The measurement is performed using an Ulbricht integrating sphere, therefore direct and diffuse reflection is summed up to yield the total reflection of the sample.

The instrument baseline is taken prior to the measurement using a white standard of the material used for the interior of the Ulbricht sphere, assuming the reflectivity of this material to be 100%.

All samples are deposited on a non-transparent substrate, resulting in zero transmission. Therefore, the absorption of the samples can be calculated from the absorption measurements by taking $A(\lambda)=(1-R(\lambda))$.

Multiplication of the $A(\lambda)$ spectrum with the spectral power distribution in a standard AM1.5 solar spectrum and integration over all wavelengths yields the totally absorbed power in the sample. The reflected power is then normalised with respect to the integrated power density in the solar spectrum (957 W/m^2).

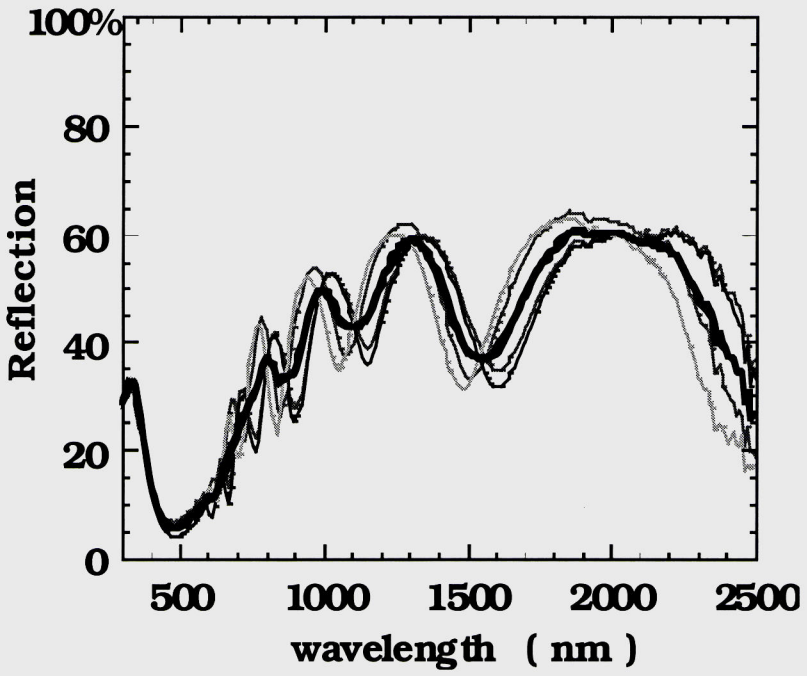

Figure 3.1: Example of reflection spectrum for one typical sample

Figure 3.1 shows a typical reflection spectrum as measured on one of the samples. Thin lines are measurements on different spots on the same sample; the thick line is the mean value at each wavelength.

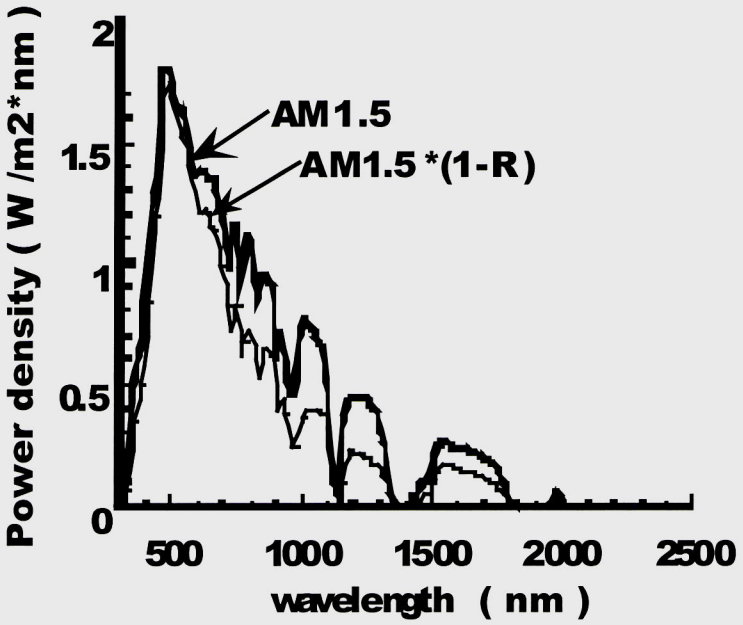

Figure 3.2: AM 1.5 spectrum measured on a typical sample

In Figure 3.2, the mean spectrum is multiplied by the AM1.5 spectrum. The total absorbed power corresponds to the surface under the curve, i.e. is obtained by integrating over all wavelengths.

3.3.1. Results

Measurements were performed on a total of 60 sample cells, which can be divided in three groups (Table 3.3):

- a selective black surface for commercial thermal absorbers was measured for comparison (reference sample R)
- the solar cells were partly of the 'superstrate' type (p-i-n on glass, samples A-E)
- the others were 'substrate' type, n-i-p cells on non-transparent substrate (samples F-K).

Sample	Type	Encapsulation	Quantity	Remark	Average of the absorbed power for all samples
Reference			4		0.95
A	p-i-n		8		0.82
B	p-i-n		8		0.9
C	p-i-n		6		0.78
D	p-i-n		4		0.89
E	p-i-n		3	same as C	0.78
F	n-i-p	none	7		0.85
G	n-i-p	none	4	tandem cell	0.74
H	n-i-p	EVA/Tefzel	6	triple cell	0.82
I	n-i-p	EVA/Tefzel	4		0.83
K	n-i-p	none	6	triple cell	0.73

Table 3.3: Absorption measured by spectrometry

More detailed values of the different samples and the measured reflection spectra are shown in the annex. The plots of the measured reflection spectra contain mean values (thick lines) as well as the multiplication of this mean curve by the AM 1.5 solar spectrum. Integration of this weighted reflectance curve over all wavelengths yields the total reflected power. Values for the absorbed power for all samples are listed in the annex.

Highest absorption (~90 %) is obtained for sample B and sample D. The other samples with p-i-n structure show absorption values that are 10 % lower, at around 80 %. An explanation for this relatively pronounced difference may be found in the use of different front and back TCO's or different contact metal. A further difference between B and D samples is the use of SnO_2 for the front TCO in B, whereas D uses ZnO.

Lowest absorption values are obtained for non-encapsulated samples G and K. These values are, however, only of academic interest as the application in a thermal collector

certainly requires encapsulation of the module. High reflectance values are explained in this case by an interferometric top TCO layer, which is optimized so as to enhance the light in-coupling for wavelengths in the photovoltaic active range (350-700 nm). Outside this range, the reflectivity increases strongly, which accounts for major reflection losses, mainly in the red and IR wavelengths region. Encapsulation of the sample with a macroscopically structured plastic foil increases the absorbed power by ~10 % absolute (Sample I), as shows the comparison between series H and K. The situation is different for Samples F. In this case, the front TCO (ZnO) is an optically thick layer, therefore no interference effects take place due to this layer, and the overall absorption of 85 % is relatively high. The encapsulation of the sample has only minor effects in this case (Sample I). There is almost no difference between non-encapsulated tandem (Sample G) and triple cells (Sample K) made by the same manufacturer, which indicates once more that the effect of a-SiGe:H alloys on the total absorbed power is negligible.

3.4. Calorimetric measurements

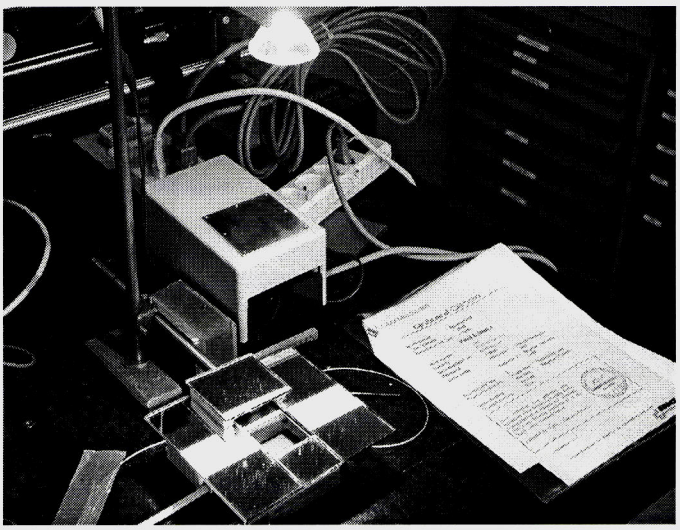

The experimental apparatus consists of a thermal flux sensor ("Episensor type A 02-050 or Peltier element of type TEC1-12714, both of a surface of 50x50 mm). As the Episensor type thermal flux sensor has an ill-defined surface, a copper plate of a thickness of 1mm has been glued onto the surface with a high thermal conductivity adhesive (Omegabond 200). The samples were then fixed on the sensitive surface with a heat conductive paste ((HTC 35SL) and illuminated according to the schema of Figure 3.5.

Figure 3.4: Photo of the absorption measures set- up by IOA

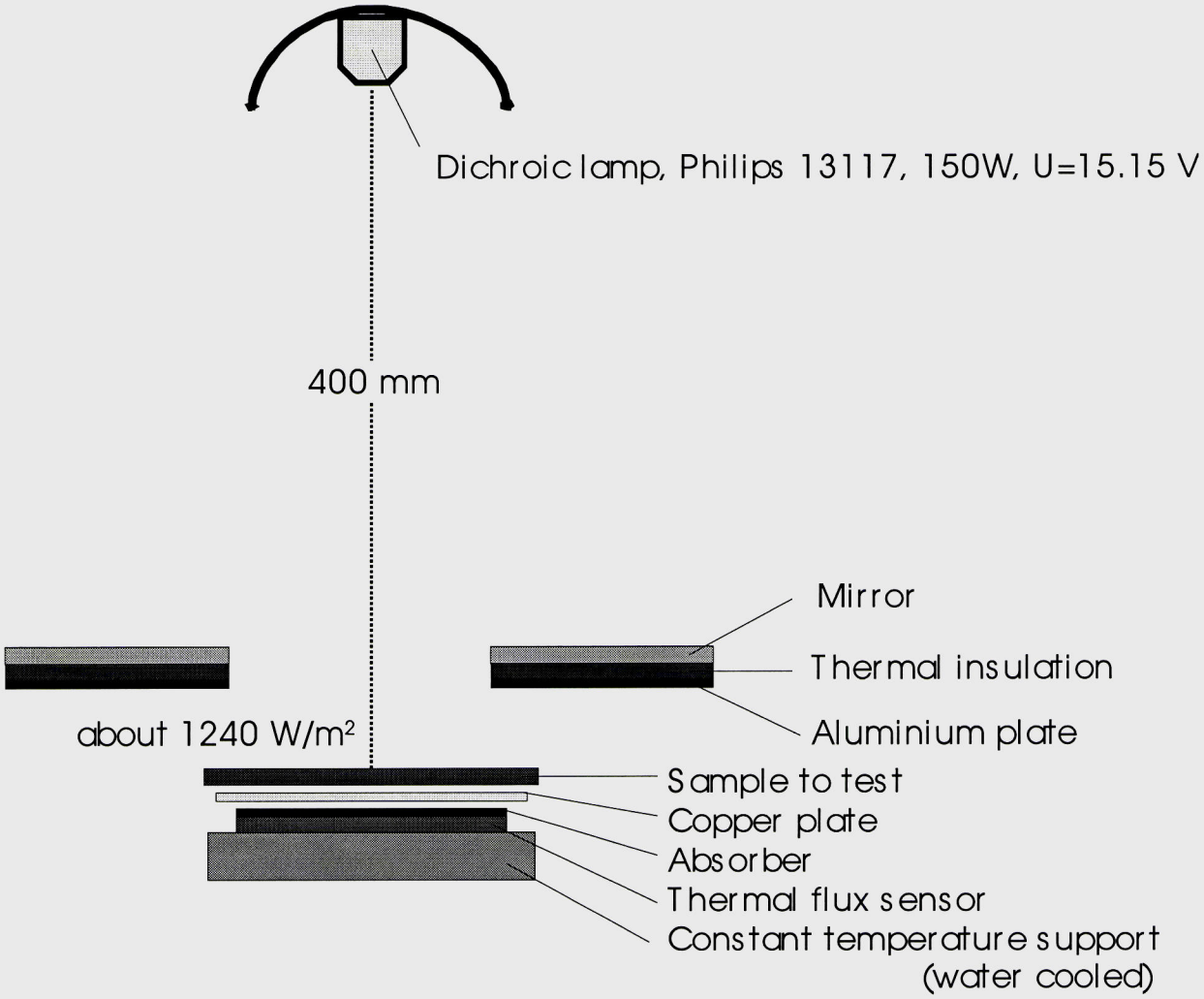

Figure 3.5: Experimental set-up

The illumination aperture was provided with the upper surface constituted with mirrors, to avoid as much as possible thermal radiation from the aperture frame to the cell under investigation. The illumination source was a Philips halogen lamp of nominal 150W, powered by a stabilised power supply under constant voltage of 15.20V, at a distance of 400 mm, which results in a fairly constant light intensity over the aperture of 20cm^2. The incident power was measured with a pyroelectric wide band laser power meter (Ophir Nova) and yields 2.48W for 20cm^2, respectively 1.99W for 16 cm^2. Each sample was measured several times and the mean value was reported in the table of Annex 8.1. No divergence larger than a few percent have been encountered.

The heat absorption of the samples was determined according to the following formula, by taking the nominal value of the black coated surface of the reference sample ($\alpha_{référence}$ = 94.0%).

$$\alpha = \alpha_{référence} (U_{epis} - U_{backgr})/(U_{ref} - U_{backgr})$$

3.4.1. Results

The results are summarized in Table 3.6. The reference sample was in principle measured prior to each series of measures and was used until the next series.

A test was performed with the reference sample (R4 + glass plate), by introducing a bare glass plate of a transmittance of 92.1%.

Sample	Type	Encapsulation	No. of samples	Average of the absorbed power for all samples
A	p-i-n		2	0.84
B	p-i-n		2	0.88
C	p-i-n		2	0.80
D	p-i-n		2	0.94
E	p-i-n		2	0.81
F	n-i-p	none	2	0.92
H	n-i-p	EVA/Tefzel	2	0.87
I	n-i-p	EVA/Tefzel	1	0.91
K	n-i-p	none	2	0.70
Reference			1	0.94

Table 3.6: Absorption measured by calorimetry

With the samples type F, tests were performed to measure the difference in absorption for the electrically unloaded and loaded cell. A clear difference in heat absorption has been detected. The generated electric power for a surface of 16 cm^2 was of 25 mW for the 56 Ohms load and a voltage of 1.195 V.

Highest absorption (~94 %) was obtained for the sample D. The absorbed power is very close to the value obtained for an optimised black absorber surface (reference: 94 %).

Lowest absorption values were obtained for non-encapsulated sample K (~70%).

3.5. Conclusion

The obtained values from the two measurement methods are quite close (see Table 3.7 and Fig. 3.8). As a conclusion, we found that quite high absorption values can be obtained for "regular" (unmodified) solar modules, which are not optimised for high optical absorption over the entire solar spectrum. In order to understand the large differences between seemingly similar structures, one would have to know the exact composition of all the layers in the stack. From the present data, it must be concluded that it is rather the encapsulation, the front TCO, and the back reflector that govern the absorption behaviour. The silicon layers seem not to have too much influence on this parameter.

No	Encapsulation	IMT	IOA	Difference absorption	Difference reflection
A	None	82%	83%	1%	1%
B	None	90%	88%	-3%	-3%
C	None	78%	80%	1%	2%
D	None	89%	94%	5%	6%
E	Lack	78%	81%	2%	3%
F	None	85%	91%	6%	8%
G	None	74%			
H	Tefzel/EVA	82%	86%	4%	4%
I	EVA/Tefzel	83%	91%	8%	10%
K	None	73%	69%	-4%	-5%
R	None	95%	94%	-1%	-1%

Table 3.7: Absorption measured by calorimetry

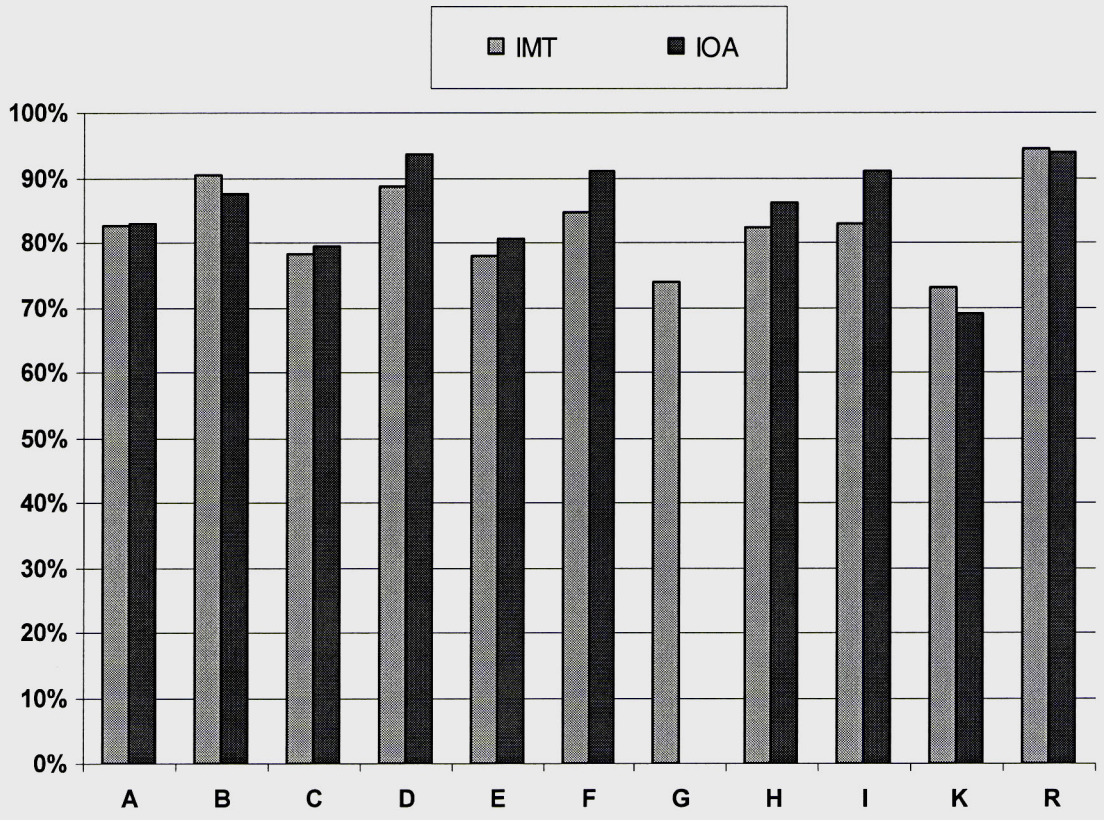

Figure 3.8: Absorption measured by calorimetry

Depending on the operating temperature of the hybrid collector, the emissivity of the sample may play a more important role and a trade-off between high optical absorption in the visible and near-IR range and a low emission coefficient in the far-IR may become necessary.

4. THERMAL STABILITY OF A-SI CELLS

4.1. Introduction

The thermal stability of PV modules used as thermal collector absorbers will directly influence their lifetime. The mean operating temperature will depend on the solar irradiation and on the system (size of the heat storage, size of the collector field). In summer, the "PV absorber" will usually experience several times stagnation temperature, which will be about 140-150°C for a non-selective absorber and 170-180°C for a selective one.

Since the PV modules are normally tested for up to 90°C, systematic information about the behaviour above this temperature is not available. A project of the Fraunhofer Institute in Freiburg ([3], [4]) show that several types of PV modules can be heated up to 150°C without any electrical and mechanical damage. Two kinds of a-Si modules (Uni-Solar and PST) were tested in the framework of this project. Both of them afforded heating up to 170°C without major damage.

For the a-Si technology, the degradation processes can be distinguished as follows:

- degradation of the junction itself,
- degradation of the encapsulation and possible destroying interactions between the encapsulation material and the thin films.

As the cell is a stack made of many layers (transparent conductive oxide/TCO, p-layer, i-layer, n-layer, back contact for a standard single junction), the degradation can be caused by:

- diffusion of one layer into the adjacent layers
- chemical reactions (oxidising, corrosion, electromigration, ...) (see [5], a study that presents problems occurring at the interface between silicon thin film conductive layers).

The degradation of the encapsulation will be strongly influenced by its properties (melting point, chemical reaction with adjacent materials, oxidising, corrosion, ...). EVA (ethyl vinyl acetate) is the most common encapsulation material used for photovoltaic modules. It becomes fluid at about 140°C and keeps on reticulating. This process is known with standard EVA, used nowadays by the module manufacturers. It is known that certain type of EVA withstands temperature better, but further material research is necessary.

The goal of the performed tests were to precisely define the operating temperature that the junction itself can withstand and to determine the junction properties that influence this behaviour. This defines the requirements for the encapsulating material.

A search in the literature [6] shows that aluminium in contact with amorphous silicium results in an interdiffusion at 180 to 210°C. This leads to a recrystallisation of the a-Si. In such a process, the aluminum will play the role of a p-dopant. This creates a device

with a strongly modified electrical behaviour. Thus, a-Si cells produced in a process that avoids joining Al-Si layers are more suited for our aims.

4.2. Testing procedure

Most samples available for this test were non-encapsulated. Since critical temperatures were not precisely known and since the number of sample modules was limited, it was decided to separate the test modules into two groups:

Sample modules to test at medium temperature during long duration (Cycles 1 to 4)

Sample modules to test at higher temperature during short duration, up to electrical breakdown (Cycle 5 to 14)

The process of measurements was done as follows:

1. Measuring the sample (I-V measurements under halogen dichroic lamps at 300 W/m^2 on the centre of the probe table)
2. Thermally cycling the sample (warming up, plateau at a given temperature level for a given duration, passively cooling down)
3. Continuing with **1.** until end of measurements or breakdown.

The complete list of performed thermal cycling is presented in Table 4.1.

Cycle No.	Duration [h]	Temp. Plateau [°C]	Current
1	10	120	-
2	10	120	-
3	80	120	-
4	100	120	-
5	1	140	-
6	1	160	-
7	1	170	-
8	10	210	-
9	10	140	17mA
10	10	170	17mA
11	50	150	17mA
12	50	150	17mA
13	50	150	17mA
14	50	150	17mA

Table 4.1:List of thermal Cycles performed

4.3. Results

With the sample modules tested at medium temperatures (Cycles 1 to 4), the goal was to confirm that operation at 120°C for long periods was not a problem. The complete list of results is presented in the Annex. Figure 4.2 shows the obtained results: each curve corresponds to the average values of a series of measurements. Only the samples type "I" did not withstand these tests. Since the same none-encapsulated cells (type "J") passed the tests, we attribute this breakdown to mechanical constraints made by thermal stress of the encapsulation. Another possible cause could be corrosion due to gases emitted from the molten the EVA.

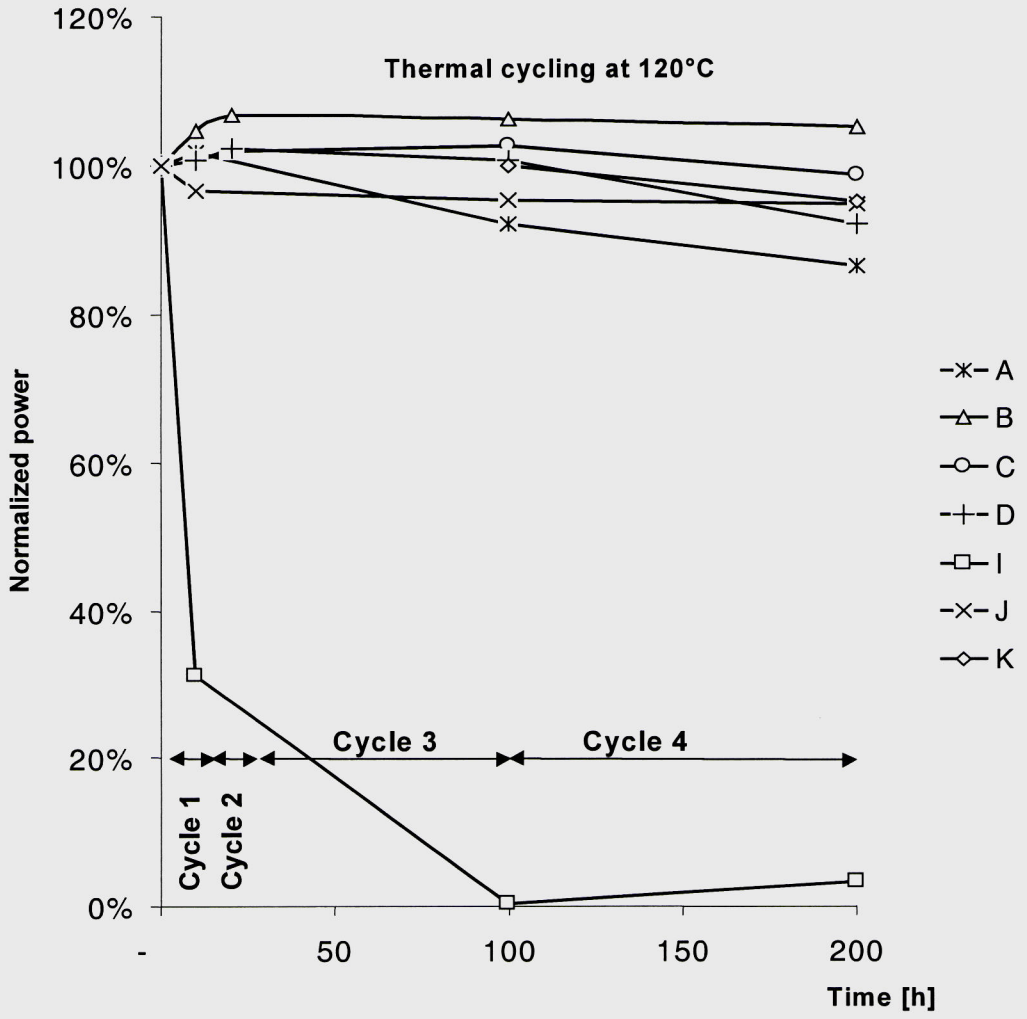

Figure 4.2: Thermal cycling of the sample modules of group A at 120°C (4 Cycles of 10, 10, 80 and 100 h)

With the second group of samples (Cycles 5 to 14), the goal was to evaluate the critical temperatures for breakdown (see fig. 4.3 concerning Cycles 5 to 8). We started therefore with 140°C during one hour (Cycle 5), then 160°C during one hour (Cycle 6), then 170°C during one hour (Cycle 7). Cycle 8 was planned to have a plateau temperature of 170°C for 10 hours, in order to confirm the results of the Cycle 7 with a longer duration. A bad operation of the temperature controller created a higher temperature: 210°C. The results of these series are nevertheless of prime interest. The results of this 210°C temperature stress series are the following:

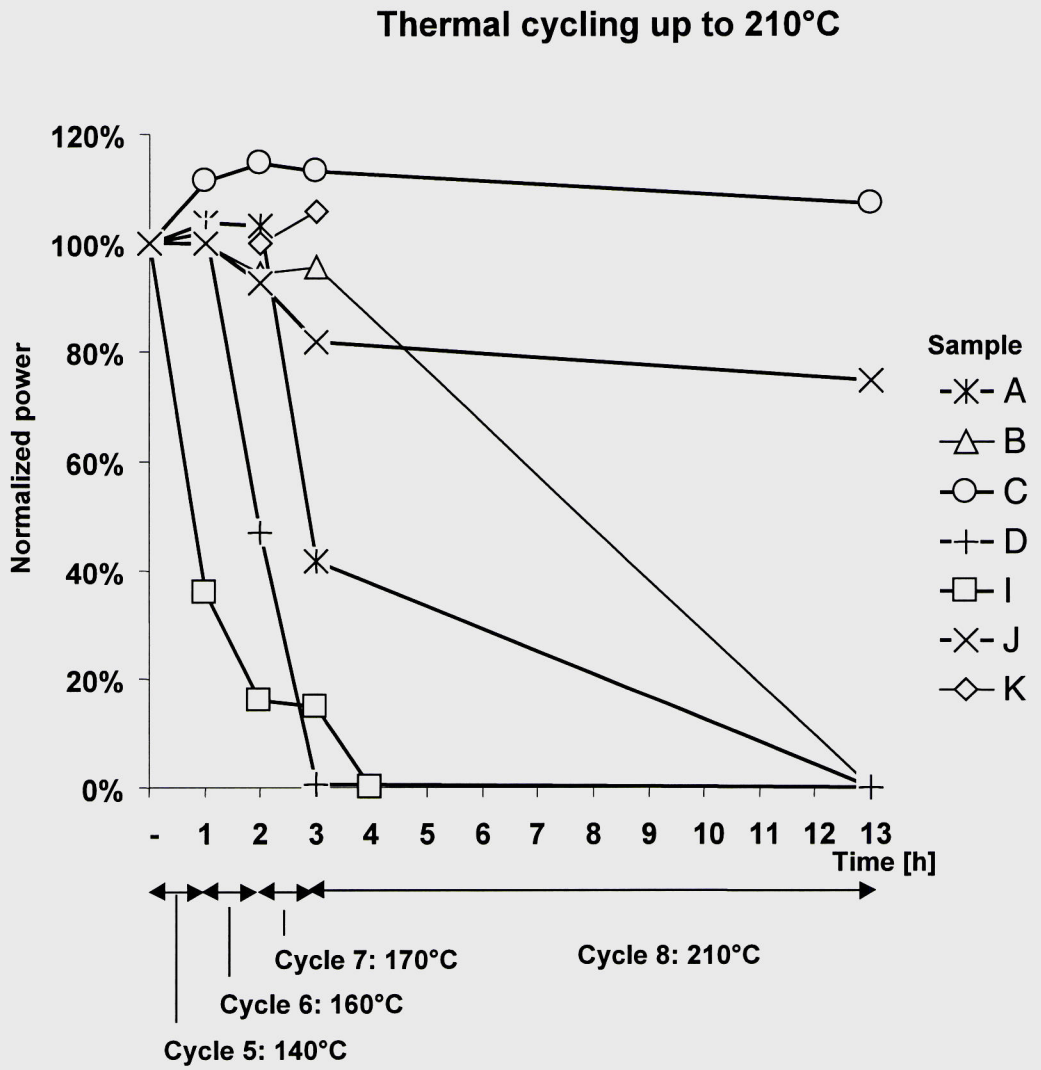

Figure 4.3: Thermal shock (up to 210°C)

- the samples type "I" did not pass Cycle 5
- the samples type "D" showed a hard degradation after Cycle 6
- the samples type "A" showed a hard degradation after Cycle 7
- the samples type "B" showed a full degradation after Cycle 8
- the samples type "J" kept their properties unchanged after Cycle 5. One notices a reduction of 20% of the efficiency after the Cycle 7. Cycle 8 was not damaging
- the samples type "C" showed no degradation all along the whole test.
- The samples of the type "K" showed no degradation after Cycle 7. For technical reasons, they were not measured after Cycle 7.

Since electromigration (transfer of molecules due to a current) is a possible cause of degradation of semi-conductors **Erreur! Source du renvoi introuvable.**, we undertook further cycling with the samples type "C" and "J" in order to check if the degradation is increased by current (Cycle 9 to 14).

We forced currents close to the nominal current into the PV device. For a reverse current, no effect were stated for cycling of up to 170°C. To force a direct current into the device means to load the parallel resistance with the nominal current. For the sample type "C", it was not possible since the voltage source was limited. For the sample type "J", the samples did pass the Cycle at 140°C for 10 hours but were destroyed after Cycle 10 at 170°C for 10 hours.

To evaluate these results, it is important to take into account the exact structure of the tested samples. Table 4.4 gives a full description of the different films and their materials.

Sample code	Substrate	TCO	thin a-Si films	back contact
A	glass	SnO_2	p-i-n	Al
B	glass	SnO_2	p / i / n / p / i / n	Al
C	glass	SnO_2	p / i / n	ITO / Cu / Ag
D	glass	SnO_2	p / i / n	Al
E	glass	SnO_2	p / i / n	ITO / Cu / Ag
Sample code	**Substrate**	**back contact**	**thin a-Si films**	**TCO**
F	polyimide	Al	n / i / p / n / i / p	ZnO/Ag paste
G	stainless steel	Ag/ZnO (?)	n / i / p / n / i / p	ITO/Ag paste
H	stainless steel	Ag/ZnO	n/i/p/n/i/p/n/i/p	ITO/carbon glue/wires
I	polyimide	Al	n / i / p / n / i / p	ZnO/Ag paste
J	polyimide	Al	n / i / p / n / i / p	ZnO/Ag paste
K	stainless steel	Ag/ZnO	n/i/p/n/i/p/n/i/p	ITO/carbon glue/wires

Table 4.4: Detailed structure of the samples

A comparison between the temperature shock test series (Fig. 4.3) and the cell contents (Table 4.4) shows that there is a relation between the presence of aluminium in the device and the stability to thermal cycling.

The best stability is obtained by type "C" samples which do not include any aluminium (contacts made of silver). The second sample having a good stability is "J" which has a back contact made of aluminium. An explanation of this stability is the following: for a n-i-p structure, the Al-back contact is deposited first. Since natural oxidising is more important for aluminium than for amorphous silicon, the resulting oxide layer between a-Si and back contact will be thicker. This oxide plays the role of an aluminium diffusion barrier. We attribute the different behaviour of the other samples to the presence of a passivation layer on the a-Si thin films, that also plays the role of a diffusion barrier (good for zinc oxyde/ZnO, bad for tin oxyde/SnO_2 and ITO).

4.4. Conclusion

A comparison between the sample modules shows very different behaviour depending on process technologies. The presence of aluminium increases the risks of pollution of the critical layers and contacts by diffusion processes. The best way to avoid such problems is to use back contacts made of silver. One has in this case an excellent stability to thermal cycling (plateau of 210°C/10h). Another possible protection is to isolate back contacts from a-Si films with oxides.

5. EMISSIVITY MEASUREMENTS

5.1. Introduction

The emissivity factor is an indication of how much power of the infrared part of the spectrum will be radiated from the photovoltaic absorber. It depends of course on the cover material. For a selective commercial solar absorber, the emissivity factor can be reduced down to 4%. For a-Si based on glass substrate, it is glass that has a high emissivity and no selectivity (absorption is equal to emissivity over the whole spectrum). The value of other encapsulation materials and of TCO are not so well known. For this reason, we completed the study with a measurement of all the tested samples and of two standard modules (Uni-Solar USS-64 and Kyocera K-120).

5.2. Results

Table 5.1 shows the detailed results. No surprise with the glazed samples: bad values between 86% and 91%.

Apparatus: INGLAS, TIR 100 (No LESO 1363)							
	Sample	Manufacturer	Encapsulation	Emitting surface	Emissivity		
Description	code	code			min	av.	max
a-Si tandem cell module	A	1	none	glass	86%	**88%**	89%
a-Si tandem cell module	B	2	resin	glass	90%	**90%**	91%
a-Si glass module	C	3	none	glass	87%	**89%**	90%
a-Si glass module	D	4	resin	glass	87%	**88%**	89%
a-Si tandem cell without encaps.	G	6	none	ITO	41%	**42%**	42%
a-Si triple cell without encapsulation	H	6	none	ITO ?	79%	**80%**	82%
a-Si tandem cell with encapsulation	I	5	EVA / EVA	EVA	82%	**86%**	89%
a-Si tandem cell without encapsulation	J	5	none	ZnO	28%	**30%**	33%
a-Si triple cell PV module (Uni-Solar)	-	-	Tefzel/EVA/Tedlar	Tefzel	95%	**95%**	95%
Polycrystalline PV module (Kyocera)	-	-	glass/EVA/Tedlar	Glass	87%	**89%**	91%

Table 5.1: Results of emissivity measurements

The Tefzel encapsulation shows an average value of $\varepsilon = 95\%$. Transparent Tedlar showed $\varepsilon = 86\%$, a bit lower than glass. Only the top layers made of TCO's have a selective property since their emissivity is reduced compared to the absorption value: $\varepsilon = 42\%$ for ITO, $\varepsilon = 30\%$ for the ZnO. (All ε figures were measured at room temperature, i.e. 293°K).

6. CONCLUSION

The aim of this studywas to verify if commercial amorphous PV modules can be directly used as absorber of a water based PV/T collector. In order to have a good thermal efficiency and a reduced risk of damage, the absorber should have sufficient absorption and must withstand a stagnation temperature of about 150°C for extended periods of time.

Absorption values of between 78% and 90% have been measured on commercially available a-Si samples. This is more than minimally required for the PV/T application.

Several samples withstood thermal cycling of 10 hours at 210°C without a significant decrease of efficiency. This excellent stability is related to the absence of aluminium.

For samples with back contacts made of aluminium, an oxidation layer acts as good protecting diffusion barrier.

As already mentioned by other R&D teams, the use of a photovoltaic module as an absorber in a thermal collector induces the loss of the spectral selectivity usually available in thermal collectors (the top layer of the module is normally non-selective). Emissivity values of different top layers were measured in the framework of this project. The standard encapsulation materials like glass, Tefzel or Tedlar have none selective and high emissivity values (between 86 and 95% depending on the layers arrangement). Only top transparent conductive oxides show a lower emissivity and thus a selective property (between 30 and 42%). However, these values are of no practical interest since the concerned samples have to be encapsulated for being used in the proposed application. They show nevertheless that the use of oxides could be an interesting way of encapsulating photovoltaic elements dedicated to use in hybrid collectors.

Further evaluation for new encapsulating or covering top layer materials should be carried our. A trade-off between a high optical absorption coefficient in the visible and near IR range and a low emission coefficient in the far IR may become necessary.

7. ACKNOWLEDGEMENTS

The work done was financially supported by the Swiss Federal Office of Energy (OFEN/BFE) represented by Mr. J. Gfeller und Mr. S. Nowak (NET AG). We would like to thank also Mr. D. Fischer, M. Götz and R. Platz from the “Institut de Microtechnique” of the University of Neuchatel for their crucial help in the framework of the two steps of this project phase. Mr. T. Sidler (Institut d’Optique Appliquée/EPFL) gave an excellent confirmation of the absorption measurements. The expertise of Mrs. A. Labouret (Solems) was particularly appreciated. Plenty of help was provided by Mr. Robin Humphry-Baker (Laboratoire de Photonique et Interfaces/EPFL). Thanks to him, too.

8. ANNEXES

8.1. Detailed test results from the absorption measurements

Summary "Absorption measurements"

Status: 18.11.98

No	Encapsulation	IMT	IOA	Difference Absorption	Difference Reflection	
R	None	95%	94%	-1%	-0.6%	low
B	None	90%	88%	-3%	-3.2%	
D	None	89%	94%	5%	5.5%	high
F	None	85%	91%	6%	7.5%	high
I	EVA/Tefzel	83%	91%	8%	9.9%	high
A	None	82%	83%	1%	0.6%	low
H	Tefzel/EVA	82%	86%	4%	4.3%	
C	None	78%	80%	1%	1.7%	low
E	Lack	78%	81%	2%	3.1%	
G	None	74%				
K	None	73%	69%	-4%	-5.4%	

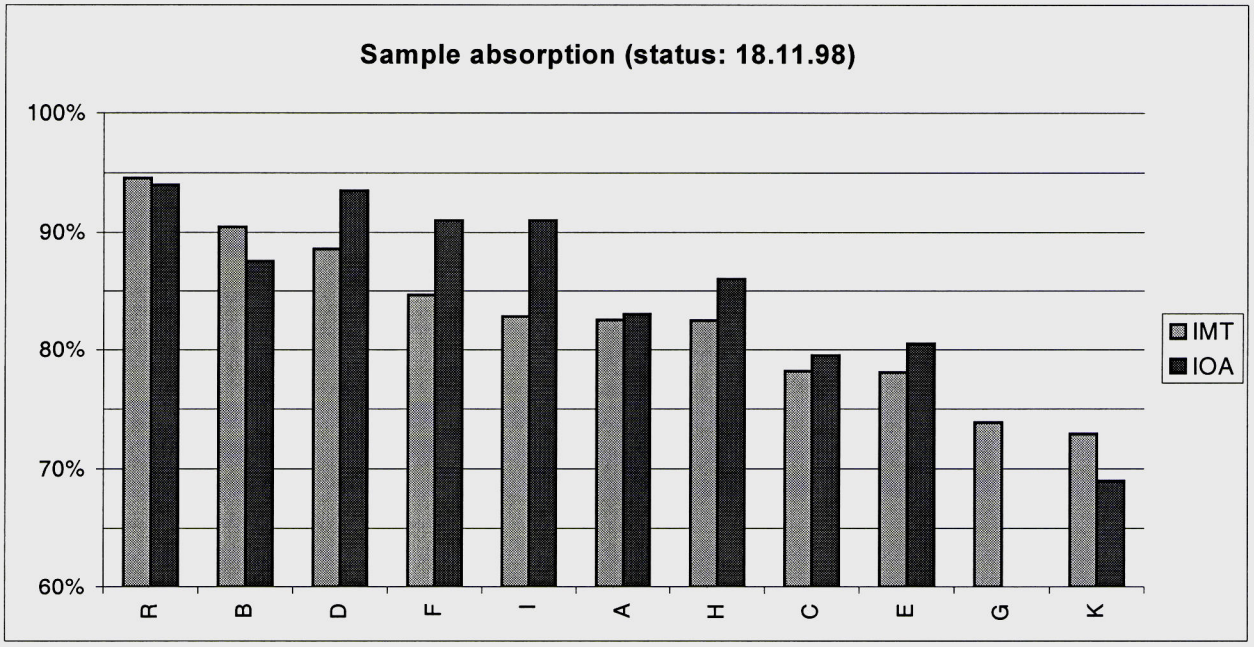

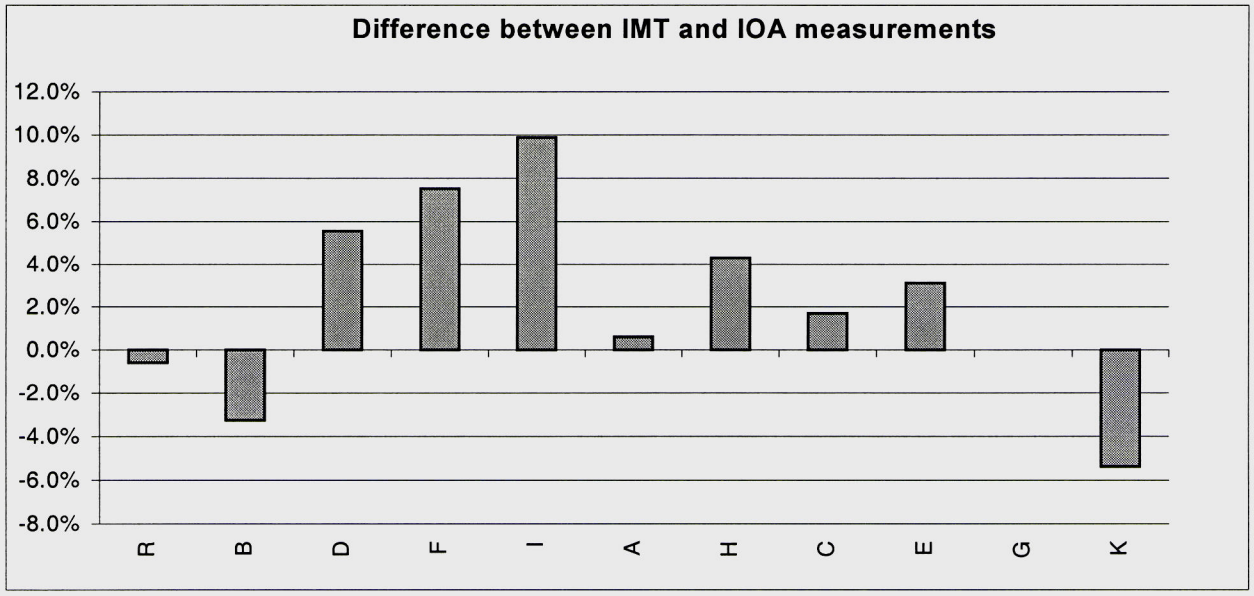

List of samples for absorption measurements (status 8.9.98)

No	Type	Encap.	Length	Width	Area	Dest.	Sent	Remark			Prefl.	Prefl./957W	absorption IMT	mean refl. absorption IMT	absorption IOA
			mm	mm	cm2										
A1		None	70	55	38.2	IMT	08.sept.98		11.09.98		168	17.6%	82.4%		
A2		None	72	65	46.8	IMT	08.sept.98		11.09.98		161	16.8%	83.2%		
A3		None	72	70	50.4	IMT	08.sept.98		11.09.98		171	17.9%	82.1%		
A4		None	65	61	39.3	IMT	08.sept.98		11.09.98		166	17.3%	82.7%		
A5		None	65	63	40.6	IMT	08.sept.98		11.09.98		168	17.6%	82.4%		
A6		None	65	55	35.2	IMT	08.sept.98		11.09.98		168	17.6%	82.4%		
A7		None	65	55	35.5	IMT	08.sept.98		11.09.98		171	17.9%	82.1%		
A8		None	70	63	43.8	IMT	08.sept.98		11.09.98		167	17.5%	82.5%	**82.5%**	
A9		None	56	51	28.6	IOA	07.sept.98								**83%**
A10		None	56	51	28.0	IOA	07.sept.98								**83%**
A11		None	304	170	516.8	ES	12.oct.98								
B1		None	78	55	42.9	IMT	08.sept.98		11.09.98		92	9.6%	90.4%		
B2		None	75	55	41.0	IMT	08.sept.98		11.09.98		90	9.4%	90.6%		
B3		None	56	53	29.1	IMT	08.sept.98		11.09.98		91	9.5%	90.5%		
B4		None	56	50	27.8	IMT	08.sept.98		11.09.98		93	9.7%	90.3%		
B5		None	57	51	29.1	IMT	08.sept.98		11.09.98		90	9.4%	90.6%		
B6		None	58	51	29.3	IMT	08.sept.98		11.09.98		91	9.5%	90.5%		
B7		None	57	51	29.1	IMT	08.sept.98		11.09.98		93	9.7%	90.3%		
B8		None	56	50	27.8	IMT	08.sept.98		11.09.98		92	9.6%	90.4%	**90.4%**	
B9		None	57	51	28.5	IOA	07.sept.98								**87%**
B10		None	57	51	28.5	IOA	07.sept.98								**88%**
B11		None	330	152	501.6	ES	12.oct.98	Labeled "SA2"							
C1	ASI 3 Oo 07/120/112 C	None	59	58	33.9	IMT	08.sept.98		08.10.98		207	21.6%	78.4%		
C2	ASI 3 Oo 07/120/112 C	None	61	56	34.2	IMT	08.sept.98		08.10.98		206	21.5%	78.5%		
C3	ASI 3 Oo 07/120/112 C	None	61	56	34.2	IMT	08.sept.98		08.10.98		208	21.7%	78.3%		
C4	ASI 3 Oo 07/120/112 C	None	59	55	32.2	IMT	08.sept.98		08.10.98		204	21.3%	78.7%		
C5	ASI 3 Oo 07/120/112 C	None	60	57	34.2	IMT	08.sept.98		08.10.98		215	22.5%	77.5%		
C6	ASI 3 Oo 07/120/112 C	None	60	56	33.3	IMT	08.sept.98		08.10.98		213	22.3%	77.7%	**78.2%**	
C7	ASI 3 Oo 07/120/112 C	None	57	53	29.9	IOA	07.sept.98								**80%**
C8	ASI 3 Oo 07/120/112 C	None	55	52	28.6	IOA	07.sept.98								**79%**
					0.0										
D1		None	60	50	30.0	IMT	08.sept.98		08.10.98		107	11.2%	88.8%		
D2		None	60	50	30.0	IMT	08.sept.98		08.10.98		113	11.8%	88.2%		
D3		None	60	50	30.0	IMT	08.sept.98		08.10.98		106	11.1%	88.9%		
D4		None	60	50	30.0	IMT	08.sept.98		08.10.98		111	11.6%	88.4%	**88.6%**	
D5		None	60	50	30.0	IOA	07.sept.98								**94%**
D6		None	60	50	30.0	IOA	07.sept.98								**93%**
D7		None	60	50	30.0	ES	12.oct.98								
D8		None	60	50	30.0	ES	12.oct.98								
E1	ASI 3 Oo 07/120/112 M	Lack	60	55	32.4	IMT	08.sept.98		08.10.98		205	21.4%	78.6%		
E2	ASI 3 Oo 07/120/112 M	Lack	60	55	32.4	IMT	08.sept.98		08.10.98		211	22.0%	78.0%		
E3	ASI 3 Oo 07/120/112 M	Lack	60	55	32.4	IMT	08.sept.98		08.10.98		214	22.4%	77.6%	**78.1%**	
E4	ASI 3 Oo 07/120/112 M	Lack	60	55	32.4	IOA	07.sept.98								**81%**
E5	ASI 3 Oo 07/120/112 M	Lack	60	55	32.4	ES	12.oct.98								**80%**

No	Type	Encap.	Length	Width	Area	Dest.	Sent	Remark			$P_{refl.}$	$P_{refl.}/957W$	absorption IMT	mean refl. absorption IMT	absorption IOA
			mm	mm	cm2										
F1	MP1.5V	None	100	37	37.0	IMT	08.sept.98		08.10.98	A: between grid	129	13.5%	86.5%		
										B: on grid	156	16.3%	83.7%		
F2	MP1.5V	None	100	37	37.0	IMT	08.sept.98		08.10.98		147	15.4%	84.6%		
F3	MP1.5V	None	100	37	37.0	IMT	08.sept.98		08.10.98		151	15.8%	84.2%		
F4	MP1.5V	None	100	37	37.0	IMT	08.sept.98		08.10.98		143	14.9%	85.1%		
F5	MP1.5V	None	100	37	37.0	IMT	08.sept.98		08.10.98		147	15.4%	84.6%		
F6	MP1.5V	None	100	37	37.0	IMT	08.sept.98		08.10.98		156	16.3%	83.7%	**84.6%**	
F7	MP1.5V	None	100	37	37.0	IOA	07.sept.98								**91%**
F8	MP1.5V	None	100	37	37.0	IOA	07.sept.98								
F9	MP1.5V	None	100	37	37.0	ES	12.oct.98	Dani's label: "1"							
F10	MP1.5V	None	100	37	37.0	ES	12.oct.98	Dani's label: "2"							
F11	MP1.5V	None	100	37	37.0	ES	12.oct.98	Dani's label: "3"							
F12	MP1.5V	None	100	37	37.0	ES	12.oct.98	Dani's label: "4"							
G1	Tandem cell	None	157	45	70.7	IMT	08.sept.98		08.10.98	A: on bar	248	25.9%	74.1%		
										B: on cell	230	24.0%	76.0%		
G2	Tandem cell	None	157	45	70.7	IMT	08.sept.98		08.10.98	A, B: different spot	258	27.0%	73.0%		
										A, B: different spot	265	27.7%	72.3%	**73.9%**	
G3	Tandem cell	None	157	45	70.7										
G4	Tandem cell	None	157	45	70.7	LESO									
H1	Triple cell	Tefzel/EVA	55	55	30.3	IMT	08.sept.98		08.10.98		165	17.2%	82.8%		
H2	Triple cell	Tefzel/EVA	55	55	30.3	IMT	08.sept.98		08.10.98		167	17.5%	82.5%		
H3	Triple cell	Tefzel/EVA	55	55	30.3	IOA	07.sept.98								**86%**
H4	Triple cell	Tefzel/EVA	55	55	30.3	IOA	07.sept.98								
H5	Triple cell	Tefzel/EVA	75	75	56.3	IMT	08.sept.98		08.10.98		171	17.9%	82.1%		
H6	Triple cell	Tefzel/EVA	95	75	71.3	IMT	08.sept.98		08.10.98		170	17.8%	82.2%		
H7	Triple cell	Tefzel/EVA	60	53	31.8	IMT	08.sept.98		08.10.98		168	17.6%	82.4%		
H8	Triple cell	Tefzel/EVA	60	52	31.2	IMT	08.sept.98		08.10.98		166	17.3%	82.7%	**82.5%**	
H9	Triple cell	Tefzel/EVA	170	130	221.0	ES	12.oct.98								
I1	MP3V	EVA/Tefzel	130	50		IMT	08.sept.98		08.10.98	A: between grid	165	17.2%	82.8%		
										B: on grid	167	17.5%	82.5%		
I2	MP3V	EVA/Tefzel	130	50		IMT	08.sept.98		08.10.98	A: between grid	149	15.6%	84.4%		
										B: on grid	177	18.5%	81.5%	**82.8%**	
I3	MP3V	EVA/Tefzel	130	50		LESO									
I4	MP3V	EVA/Tefzel	130	50		IOA	08.sept.98								**91%**

No	Type	Encap.	Length	Width	Area	Dest.	Sent	Remark			$P_{refl.}$	$P_{refl./957W}$	absorption IMT	mean refl. absorption IMT	absorption IOA
			mm	mm	cm2										
K1	Triple cell	None	81	70	56.7			0.4536							
K2	Triple cell	None	81	60	48.3	IMT	12.oct.98		19.10.98	A: deep blue	247	25.8%	74.2%		
										B: close to bus	268	28.0%	72.0%		
K3	Triple cell	None	80	60	47.6										
K4	Triple cell	None	70	60	41.7										
K5	Triple cell	None	80	50	39.6	IMT	12.oct.98		19.10.98	A: deep blue	257	26.9%	73.1%		
										B: close to bus	272	28.4%	71.6%		
K6	Triple cell	None	60	59	35.4										
K7	Triple cell	None	61	60	36.0										
K8	Triple cell	None	70	49	34.3	IMT	12.oct.98		19.10.98		247	25.8%	74.2%		
K9	Triple cell	None			0.0										
K10	Triple cell	None	58	50	29.0	IMT	12.oct.98		19.10.98		264	27.6%	72.4%	**72.9%**	
K11	Triple cell	None	60	50	30.0										
K12	Triple cell	None	61	50	29.9	IOA									**69%**
K13	Triple cell	None	50	50	24.8	IOA									
K14	Triple cell	None	240	180	432.0	ES	12.oct.98								
R1	Chrome oxyde		73	73	53.3	IMT	08.sept.98		08.10.98	A,B: different spots	52	5.4%	94.6%		
										A,B: different spots	54	5.6%	94.4%		
R2	Chrome oxyde		77	74	57.0	IMT	08.sept.98		08.10.98	A,B: different spots	53	5.5%	94.5%		
										A,B: different spots	49	5.1%	94.9%	**94.6%**	
R3	Chrome oxyde		77	73	55.8	ES	08.sept.98								
R4	Chrome oxyde		54	50	27.0	IOA	07.sept.98								**94%**
R5	Chrome oxyde		23	22	5.1	IOA	07.sept.98								
R6	Chrome oxyde		26	23	5.9										

List of samples for absorption measurements (status: 8.9.98)

No	Encap.	Length	Width	Area	Testing	Sent	Prefl.	Prefl./957W	mean refl. power		Emissivity	Material
		mm	mm	cm2			W/m2					
A1	None	70	55	38.2	IMT	08.sept.98	168	17.6%				
A2	None	72	65	46.8	IMT	08.sept.98	161	16.8%				
A3	None	72	70	50.4	IMT	08.sept.98	171	17.9%				
A4	None	65	61	39.3	IMT	08.sept.98	166	17.3%				
A5	None	65	63	40.6	IMT	08.sept.98	168	17.6%				
A6	None	65	55	35.2	IMT	08.sept.98	168	17.6%				
A7	None	65	55	35.5	IMT	08.sept.98	171	17.9%				
A8	None	70	63	43.8	IMT	08.sept.98	167	17.5%	17.5%			
A9	None	56	51	28.6	IOA	07.sept.98				83		
A10	None	56	51	28.0	IOA	07.sept.98				83		
A11	None	304	170	516.8	ES	12.oct.98					0.85	Glass

Measured absoprtion coefficient (average) **82** **83**

Graphs of the measurements

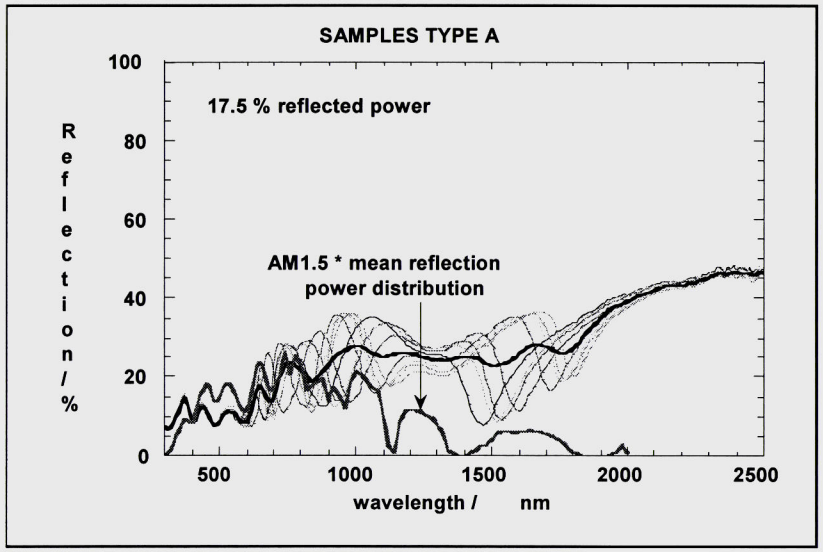

Interpretation

Encapsulation does not influence the absorption in the case of p-i-n solar cells (encapsulation on back side), whereas it does have an influence for n-i-p type cells (encapsulation on illuminated side).
The plots furthermore contain mean values (thick lines) as well as the multiplication of this mean curve with the AM 1.5 solar spectrum. Integration of this weighted reflectance curve over all wavelengths yields the total reflected power. Values for the absorbed power are listed in table above.
Highest absorption (~90 %) is obtained for the samples type B & D. The absorbed power is quite close to the value obtained for an optimized black absorber surface (95 %). The samples type A in the p-i-n structure show absorptions that are 10 % absolute lower, at around 80 %.
An explanation for this relatively pronounced difference may be found in the use of different front and back TCOs or the back contact metal.

List of samples for absorption measurements (status: 8.9.98)

No	Encap.	Length	Width	Area	Testing	Sent	Prefl.	Prefl./957W	mean refl. powe		Emissivity	Material
		mm	mm	cm2			W/m2					
B1	None	78	55	42.9	IMT	08.sept.98	92	9.6%				
B2	None	75	55	41.0	IMT	08.sept.98	90	9.4%				
B3	None	56	53	29.1	IMT	08.sept.98	91	9.5%				
B4	None	56	50	27.8	IMT	08.sept.98	93	9.7%				
B5	None	57	51	29.1	IMT	08.sept.98	90	9.4%				
B6	None	58	51	29.3	IMT	08.sept.98	91	9.5%				
B7	None	57	51	29.1	IMT	08.sept.98	93	9.7%				
B8	None	56	50	27.8	IMT	08.sept.98	92	9.6%	9.6%			
B9	None	57	51	28.5	IOA	07.sept.98				87		
B10	None	57	51	28.5	IOA	07.sept.98				88		
B11	None	330	152	501.6	ES	12.oct.98					0.85	Glass
Measured absorption coefficient (average)									90	88		

Graphs of the measurements

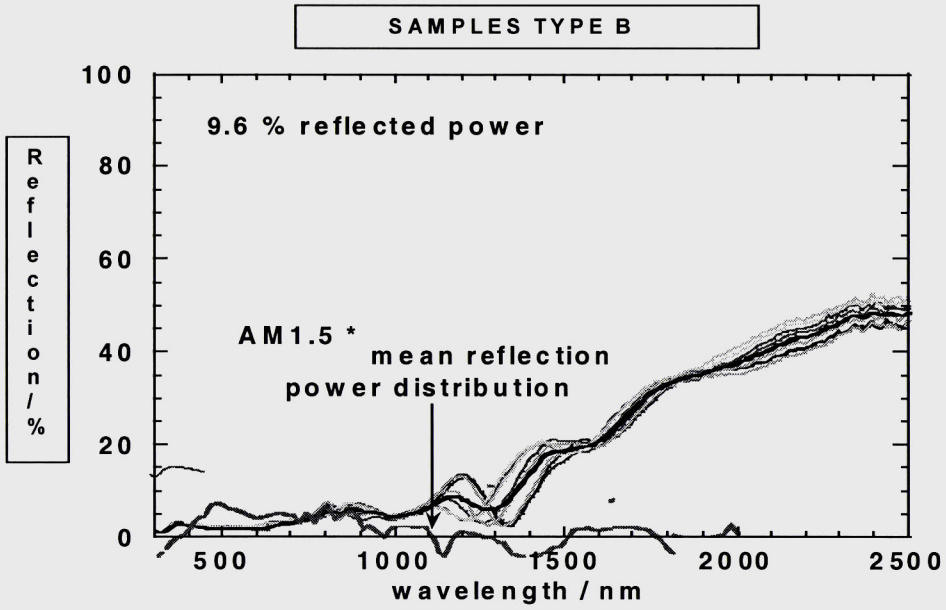

Interpretation

A high absorption (~90 %) is obtained for the samples type B. The absorbed power is quite close to the value obtained for an optimized black absorber surface (95 %). An explanation for this relatively pronounced difference to the other samples may be found in the use of different front and back TCOs or the back contact metal. These samples contain a-SiGe:H alloys with a lower optical gap and therefore enhanced optical absorption. It is, however, not clear, to what extent this fact is responsible for the enhanced absorption. A further difference between the samples is the use of SnO2 as front TCO in by Solarex, whereas other manufacturer uses ZnO.

List of samples for absorption measurements (status:

No	Encap.	Length	Width	Area	Testing	Sent	Prefl.	Prefl./957W	mean refl. power		Emissivity	Material
		mm	mm	cm2			W/m2					
C1	None	59	58	33.9	IMT	08.sept.98	207	21.6%				
C2	None	61	56	34.2	IMT	08.sept.98	206	21.5%				
C3	None	61	56	34.2	IMT	08.sept.98	208	21.7%				
C4	None	59	55	32.2	IMT	08.sept.98	204	21.3%				
C5	None	60	57	34.2	IMT	08.sept.98	215	22.5%				
C6	None	60	56	33.3	IMT	08.sept.98	213	22.3%	21.8%			
C7	None	57	53	29.9	IOA	07.sept.98				80		
C8	None	55	52	28.6	IOA	07.sept.98				79		
						Measured absorption coefficient (average)				78		80
E1	Lack	60	55	32.4	IMT	08.sept.98	205	21.4%				
E2	Lack	60	55	32.4	IMT	08.sept.98	211	22.0%				
E3	Lack	60	55	32.4	IMT	08.sept.98	214	22.4%	21.9%			
E4	Lack	60	55	32.4	IOA	07.sept.98				81		
E5	Lack	60	55	32.4	ES	12.oct.98				80	0.83	Glass
						Measured absorption coefficient (average)				78		81

Graphs of the measurements

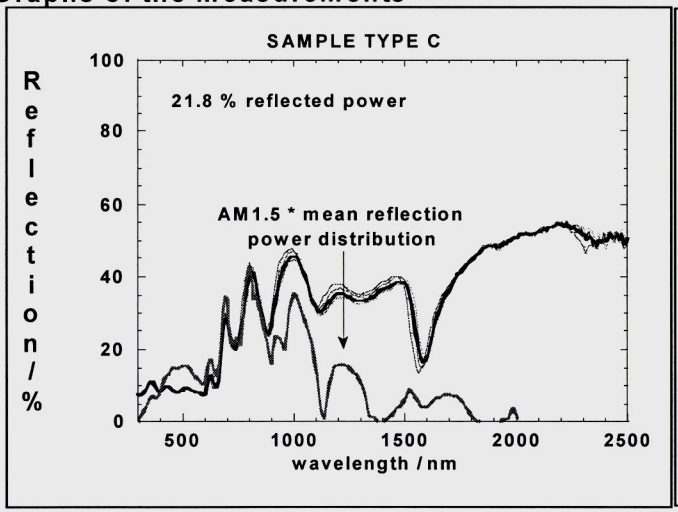

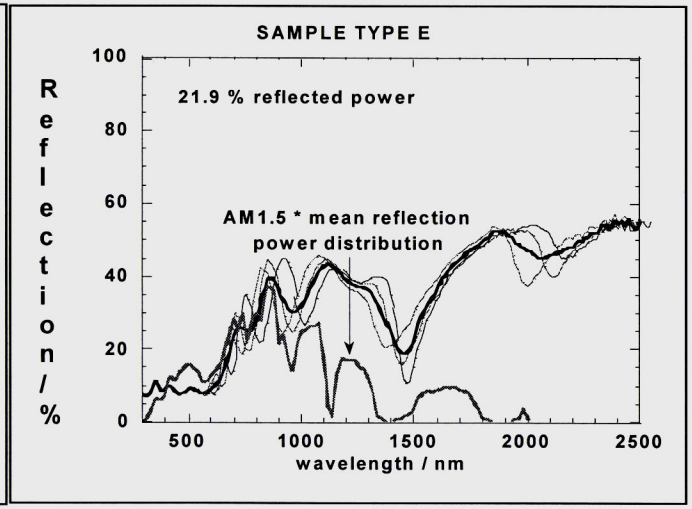

Interpretation

Encapsulation does not influence the absorption in the case of p-i-n solar cells (encapsulation on back side), whereas it does have an influence for n-i-p type cells (encapsulation on illuminated side).

The measured reflection spectra are shown in the annex. The plots furthermore contain mean values (thick lines) as well multiplication of this mean curve with the AM 1.5 solar spectrum Integration of this weighted reflectance curve over all yields the total reflected power. Values for the absorbed power are listed in table

These samples in the p-i-n structure show absorptions that are 10 % absolute lower, at around 80 %. An explanation for thi relatively pronounced difference may be found in the use different front and back TCOs or the back contact metal.

List of samples for absorption measurements (status: 8.9.98)

No	Encap.	Length	Width	Area	Testing	Sent	Prefl.	Prefl./957W	mean refl. power		Emissivity	Material
		mm	mm	cm2			W/m2					
D1	None	60	50	30.0	IMT	08.sept.98	107	11.2%				
D2	None	60	50	30.0	IMT	08.sept.98	113	11.8%				
D3	None	60	50	30.0	IMT	08.sept.98	106	11.1%				
D4	None	60	50	30.0	IMT	08.sept.98	111	11.6%	11.4%			
D5	None	60	50	30.0	IOA	07.sept.98				94		
D6	None	60	50	30.0	IOA	07.sept.98				93		
D7	None	60	50	30.0	ES	12.oct.98					0.82	Glass
D8	None	60	50	30.0	ES	12.oct.98					0.81	Glass

Measured absorption coefficient (average) 90 88

Graphs of the measurements

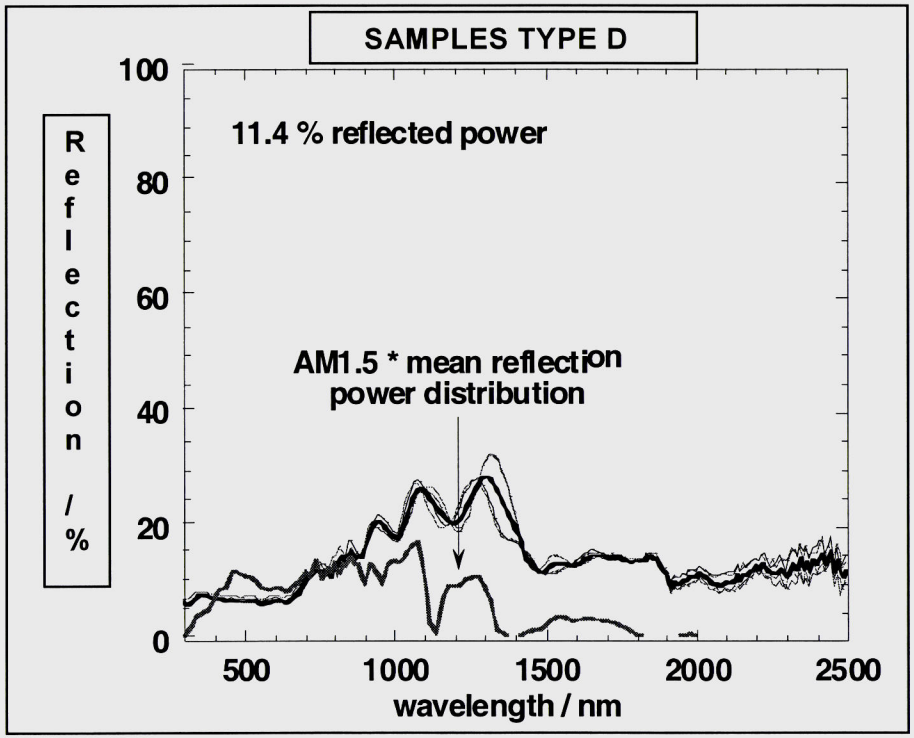

Interpretation

Encapsulation does not influence the absorption in the case of p-i-n solar cells (encapsulation on back side), whereas it does have an influence for n-i-p type cells (encapsulation on illuminated side).

The measured reflection spectra are shown in the annex. The plots furthermore contain mean values (thick lines) as well as the multiplication of this mean curve with the AM 1.5 solar spectrum. Integration of this weighted reflectance curve over all wavelengths yields the total reflected power. Values for the absorbed power are listed in table above.

Highest absorption (~90 %) is obtained for samples type B & D. The absorbed power is quite close to the value obtained for an optimized black absorber surface (Reference with 95 %). The other samples in the p-i-n structure show absorptions that are 10 % absolute lower, at around 80 %. An explanation for this relatively pronounced difference may be found in the use of different front and back TCOs or the back contact metal.

The samples contain a-SiGe:H alloys with a lower optical gap and therefore enhanced optical absorption. It is, however, not clear, to what extent this fact is responsible for the enhanced absorption, especially as the Intersolar sample does not contain a-SiGe:H alloys. A further differen between the type B and type D samples is the use of SnO2 as front TCO by B, whereas D uses ZnO.

List of samples for absorption measurements

No	Type	Encaps.	Length	Width	Area	Testing	Sent		Prefl.	Prefl./957W	mean refl. power		Emissivity	Material
			mm	mm	cm2				W/m2					
G1	Tandem cell	None	157	45	70.7	IMT	08.sept.98	A: on bar	248	25.9%				
								B: on cell	230	24.0%				
G2	Tandem cell	None	157	45	70.7	IMT	08.sept.98	A, B: different spots	258	27.0%				
								A, B: different spots	265	27.7%	26.1%			
G3	Tandem cell	None	157	45	70.7									
G4	Tandem cell	None	157	45	70.7	LESO								
							Measured absorption coefficient (average)				74			
H1	Triple cell	Tefzel/EVA	55	55	30.3	IMT	08.sept.98		165	17.2%				
H2	Triple cell	Tefzel/EVA	55	55	30.3	IMT	08.sept.98		167	17.5%				
H3	Triple cell	Tefzel/EVA	55	55	30.3	IOA	07.sept.98					86		
H4	Triple cell	Tefzel/EVA	55	55	30.3	IOA	07.sept.98					86		
H5	Triple cell	Tefzel/EVA	75	75	56.3	IMT	08.sept.98		171	17.9%				
H6	Triple cell	Tefzel/EVA	95	75	71.3	IMT	08.sept.98		170	17.8%				
H7	Triple cell	Tefzel/EVA	60	53	31.8	IMT	08.sept.98		168	17.6%				
H8	Triple cell	Tefzel/EVA	60	52	31.2	IMT	08.sept.98		166	17.3%	17.5%			
H9	Triple cell	Tefzel/EVA	170	130	221.0	ES	12.oct.98						0.87	Tefzel
							Measured absorption coefficient (average)				82	86		
K1	Triple cell	None	81	70	56.7									
K2	Triple cell	None	81	60	48.3	IMT	12.oct.98	A: deep blue	247	25.8%				
								B: close to bus	268	28.0%				
K3	Triple cell	None	80	60	47.6									
K4	Triple cell	None	70	60	41.7									
K5	Triple cell	None	80	50	39.6	IMT	12.oct.98	A: deep blue	257	26.9%				
								B: close to bus	272	28.4%				
K6	Triple cell	None	60	59	35.4									
K7	Triple cell	None	61	60	36.0									
K8	Triple cell	None	70	49	34.3	IMT	12.oct.98		247	25.8%				
K9	Triple cell	None			0.0									
K10	Triple cell	None	58	50	29.0	IMT	12.oct.98		264	27.6%	27.1%			
K11	Triple cell	None	60	50	30.0							69		
K12	Triple cell	None	61	50	29.9	IOA						69		
K13	Triple cell	None	50	50	24.8	IOA								
K14	Triple cell	None	240	180	432.0	ES	12.oct.98						0.81	ITO
							Measured absorption coefficient (average)				73	69		

Graphs of the measurements

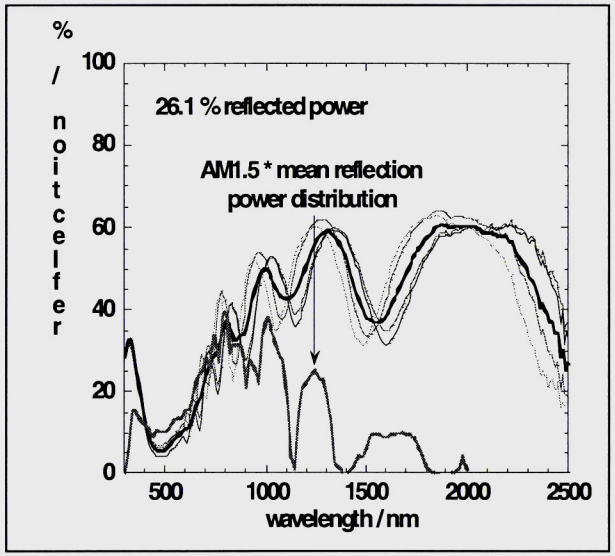

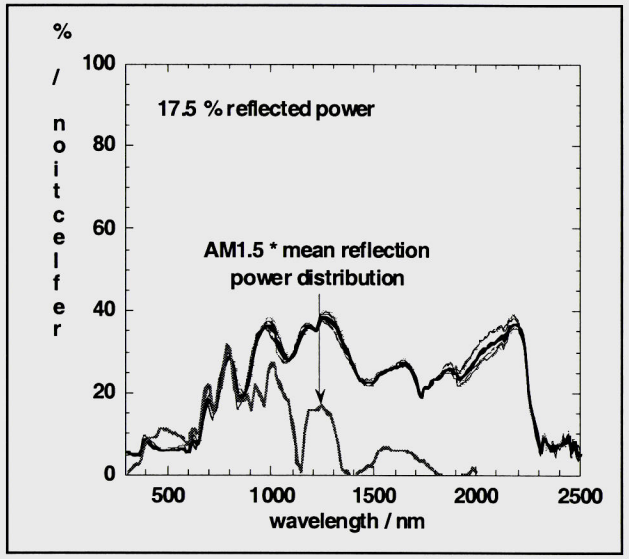

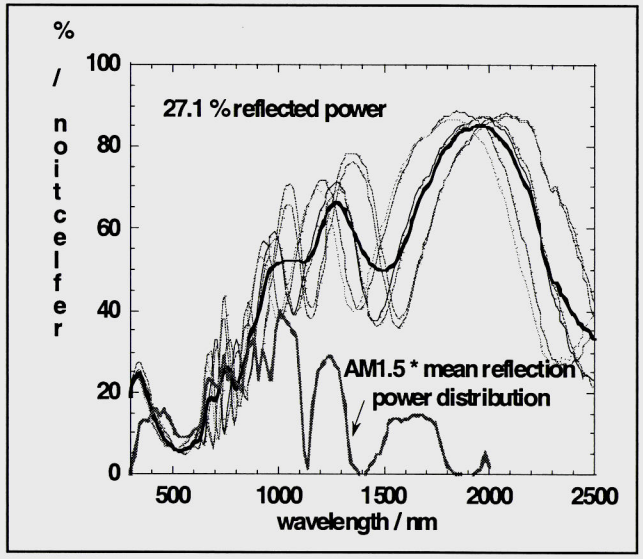

Interpretation

The plots furthermore contain mean values (thick lines) as well as the multiplication of this mean curve with the AM 1.5 solar spectrum. Integration of this weighted reflectance curve over all wavelengths yields the total reflected power. Values for the absorbed power are listed in table above. Lowest absorption values are obtained for non-encapsulated samples type G & K. These values are, however, only of academic interest as the application in a thermal collector certainly requires encapsulation of the module. High reflectance values are explained in this case by an interferometric top TCO layer, which is optimized so as to enhance the light in-coupling for wavelengths in the photovoltaic active range (350-700 nm). Outside this range the reflectivity increases strongly, which accounts for important reflection losses, mainly in the red and IR wavelengths region. Encapsulation of the sample with a macroscopically structured plastic foil increases the absorbed power by ~10 % absolute, as shows the comparison between series H and K. The situation is different for the samples type F. In this case, the front TCO (ZnO) is an optically thick layer, therefore no interference effects take place due to this layer and the overall absorption of 85 % is relatively high. The encapsulation of the sample type F has only minor influences in this case. There is almost no difference between non-encapsulated tandem and triple cells (type G & H), indicating once more that the effect of a-SiGe:H alloys on the total absorbed power is negligible

NEW GENERATION OF HYBRID SOLAR COLLECTORS

List of samples for absorption measurements (status: 8.9.98)

									Measurements IMT			Mes. IOA	Mes. Schweizer
No	Type	Encaps.	Length	Width	Area	Testing	Sent		Prefl.	Prefl./957W	mean refl. power		Emissivity
			mm	mm	cm2				W/m2				
F1	MP1.5V	None	100	37	37.0	IMT	8-Sep-98	A: between grid	129	13.5%			
								B: on grid	156	16.3%			
F2	MP1.5V	None	100	37	37.0	IMT	8-Sep-98		147	15.4%			
F3	MP1.5V	None	100	37	37.0	IMT	8-Sep-98		151	15.8%			
F4	MP1.5V	None	100	37	37.0	IMT	8-Sep-98		143	14.9%			
F5	MP1.5V	None	100	37	37.0	IMT	8-Sep-98		147	15.4%			
F6	MP1.5V	None	100	37	37.0	IMT	8-Sep-98		156	16.3%	15.4%		
F7	MP1.5V	None	100	37	37.0	IOA	8-Sep-98					91	
F8	MP1.5V	None	100	37	37.0	IOA	7-Sep-98					91	
F9	MP1.5V	None	100	37	37.0	ES	12-Oct-98	Samples to small to be measured separately!					0.38
F10	MP1.5V	None	100	37	37.0	ES	12-Oct-98	"					0.38
F11	MP1.5V	None	100	37	37.0	ES	12-Oct-98	"					0.36
F12	MP1.5V	None	100	37	37.0	ES	12-Oct-98	"					0.36
								Measured absorption coefficient (average)			85	91	
I1	MP3V	EVA/Tefzel	130	50		IMT	8-Sep-98	A: between grid	165	17.2%			
								B: on grid	167	17.5%			
I2	MP3V	EVA/Tefzel	130	50		IMT	8-Sep-98	A: between grid	149	15.6%			
								B: on grid	177	18.5%	17.2%		
I3	MP3V	EVA/Tefzel	130	50		LESO							
I4	MP3V	EVA/Tefzel	130	50		IOA	8-Sep-98					91	
								Measured absorption coefficient (average)			83	91	

Graphs of the measurements

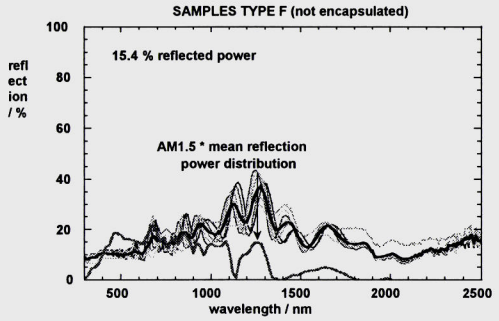

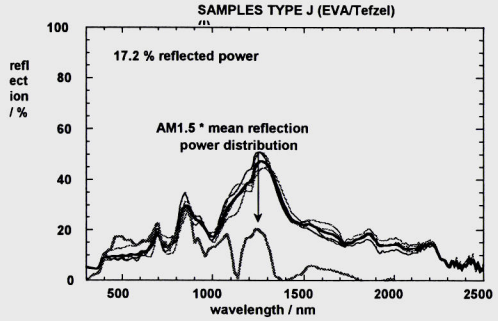

Interpretation

The plots contain mean values (thick lines) as well as the multiplication of this mean curve with the AM 1.5 solar spectrum. Integration of this weighted reflectance curve over all wavelengths yields the total reflected power. Values for the absorbed power are listed in table above.
By the sample type F & I, the front TCO (ZnO) is an optically thick layer, therefore no interference effects take place due to this layer and the overall absorption of 85 % is relatively high.
The encapsulation has only minor influences in this case.

8.2. Detailed results of high temperature cycling measurements

Manufacturer 1 / Sample A

No.	Area	Cycle No.	Isc	Uoc	Pmax	FF	Eff	Rs	Rsh	G	Tmod
	cm2		mA	V	W	%	%	Ohm	Ohm	W/m2	°C
A.1	930	-	83.8	20.8	1.07	3.9%	61.5%	2261	57.6	299	30.2
A.1	930	8	61.1	13.8	0.27	1.0%	32.7%	277	147.0	298	16.0
A.2	930	-	90.3	20.9	1.20	4.3%	63.3%	2529	23.4	298	30.6
A.2	930	-	90.2	20.8	1.19	4.3%	63.7%	2349	24.3	297	32.7
A.2	930	5	89.4	21.7	1.23	4.4%	63.5%	2743	23.3	301	27.6
A.2	930	5	89.6	21.4	1.22	4.4%	63.4%	2754	22.0	300	30.4
A.2	930	6	89.3	21.8	1.21	4.3%	62.1%	2766	25.9	302	25.4
A.2	930	6	89.8	21.6	1.21	4.3%	62.4%	2805	23.5	301	27.6
A.2	930	7	87.9	16.8	0.63	2.3%	42.5%	876	76.7	297	28.3
A.2	930	7	87.9	17.1	0.64	2.3%	42.6%	800	76.7	298	29.1
A.3	930	-	89.9	20.3	0.96	3.5%	52.8%	1040	36.8	301	29.4
A.3	930	-	90.0	20.2	0.96	3.5%	53.0%	1053	36.0	300	30.8
A.3	930	5	89.1	20.8	1.02	3.6%	54.7%	1139	37.3	300	25.6
A.3	930	5	89.3	20.7	1.01	3.6%	54.9%	1148	34.6	300	27.7
A.3	930	6	90.1	21.0	1.02	3.7%	53.6%	1066	28.2	299	27.1
A.3	930	6	90.4	20.9	1.02	3.6%	53.9%	1065	34.3	303	29.7
A.3	930	7	77.9	12.4	0.30	1.1%	31.3%	234	113.5	298	27.8
A.3	930	7	77.9	12.4	0.30	1.1%	31.4%	231	111.2	298	28.5
A.3	930	7	78.0	12.7	0.31	1.1%	31.4%	256	111.6	298	30.4
A.4	930	-	90.7	21.4	1.19	4.3%	61.1%	1908	29.9	299	26.0
A.4	930	-	90.8	21.2	1.18	4.2%	61.4%	1832	28.6	299	28.9
A.4	930	1	90.0	21.5	1.20	4.3%	61.8%	1845	28.9	301	25.0
A.4	930	1	87.4	21.3	1.08	3.9%	58.2%	1878	30.6	301	27.2
A.4	930	2/ 3	89.7	20.9	1.13	4.0%	60.4%	2583	33.2	302	32.3
A.4	930	2/ 3	89.8	20.9	1.13	4.0%	60.3%	1876	33.2	301	33.0
A.4	930	4	89.0	21.2	1.03	3.7%	54.6%	1271	47.7	298	27.8
A.4	930	4	89.4	21.0	1.03	3.7%	54.8%	1267	48.2	298	28.3
A.5	930	-	90.0	21.8	1.26	4.5%	64.1%	1867	26.1	299	26.2
A.5	930	-	90.0	21.6	1.25	4.5%	64.2%	1854	25.1	299	28.5
A.5	930	-	90.1	21.4	1.24	4.5%	64.3%	2140	24.1	299	30.1
A.5	930	1	88.3	21.7	1.29	4.6%	67.4%	2406	22.6	300	27.5
A.5	930	1	88.4	21.5	1.28	4.6%	67.6%	2405	21.4	300	29.4
A.5	930	2/ 3	90.4	21.5	1.11	4.0%	57.3%	1837	37.1	301	28.2
A.5	930	2/ 3	90.2	21.2	1.11	4.0%	58.0%	3182	33.2	301	30.6
A.5	930	2/ 3	91.6	21.3	1.13	4.0%	57.9%	1900	34.6	304	27.6
A.5	930	2/ 3	92.1	20.8	1.11	3.9%	57.8%	1778	34.7	305	33.5
A.5	930	4	89.5	21.4	1.08	3.9%	56.7%	1583	44.3	299	29.4
A.6	930	-	86.5	21.0	1.05	3.8%	57.9%	1779	36.0	299	28.8

Manufacturer 2 / Sample B

No.	Area	Cycle No.	Isc	Uoc	Pmax	FF	Eff	Rs	Rsh	G	Tmod
	cm2		mA	V	W	%	%	Ohm	Ohm	W/m2	°C
B.1	495	-	95.5	10.8	0.62	4.2%	60.5%	1058	18.8	300	28.9
B.1	495	-	96.3	10.6	0.62	4.2%	60.9%	1045	18.0	301	34.2
B.2	495	-	94.9	10.5	0.62	4.2%	62.5%	1005	16.9	299	36.9
B.2	495	1	93.7	11.0	0.65	4.4%	63.3%	1193	20.2	301	27.0
B.2	495	1	94.0	10.9	0.65	4.4%	63.4%	1174	19.4	300	29.1
B.2	495	2	94.5	10.9	0.66	4.5%	64.3%	1723	21.1	299	28.1
B.2	495	2	95.1	10.8	0.66	4.4%	64.0%	1632	15.9	299	31.8
B.2	495	3	94.3	11.1	0.66	4.3%	63.3%	1167	22.3	309	25.7

B.2	495	3	94.3	10.9	0.66	4.4%	63.9%	1070	21.2	305	30.0
B.2	495	4	93.2	11.1	0.65	4.4%	63.1%	1538	19.0	299	27.9
B.2	495	4	93.6	11.0	0.65	4.4%	63.0%	1324	19.0	298	29.4
B.3	495	-	94.8	10.7	0.66	4.4%	64.9%	1646	15.4	300	29.9
B.3	495	-	94.8	10.7	0.66	4.4%	64.9%	1716	15.6	300	31.7
B.3	495	5	94.8	10.8	0.66	4.4%	64.1%	1662	17.0	304	27.6
B.3	495	B.1	94.9	10.8	0.65	4.4%	64.1%	1711	17.2	303	29.5
B.3	495	6	95.1	10.5	0.62	4.2%	62.8%	1752	18.5	299	38.1
B.3	495	6	95.4	10.4	0.62	4.2%	62.6%	1611	18.8	299	41.0
B.3	495	6	95.4	10.4	0.62	4.2%	62.6%	1641	18.8	299	42.0
B.3	495	7	93.2	10.8	0.63	4.2%	62.6%	1840	22.8	301	30.1
B.3	495	7	93.2	10.7	0.63	4.2%	62.6%	1825	19.0	298	32.0

Manufacturer 3 / Sample C

No.	Area	Cycle No.	Isc	Uoc	Pmax	Eff.	FF	Rp	Rs	G	Tamb
	cm2		mA	V	W	%	%	Ohm	Ohm	W/m2	°C
C.1	132	-	20.6	10.9	0.15	3.9%	68.3%	4935	42.4	301	28.2
C.1	132	-	20.7	10.9	0.15	3.9%	68.1%	4789	40.8	301	29.9
C.1	132	5	20.6	10.9	0.15	3.9%	68.4%	5824	45.2	301	28.2
C.1	132	5	20.7	10.9	0.15	3.9%	68.1%	4330	43.5	301	29.9
C.1	132	6	20.6	11.1	0.16	4.1%	70.9%	5492	94.9	303	26.1
C.1	132	6	20.7	11.0	0.16	4.0%	70.7%	6868	37.6	302	30.2
C.1	132	6	20.7	10.9	0.16	4.0%	70.4%	6290	43.1	302	33.5
C.1	132	7	20.0	11.1	0.16	4.0%	71.8%	13686	55.0	299	29.6
C.1	132	7	20.0	11.0	0.16	4.0%	72.1%	24716	52.8	298	29.2
C.1	132	7	20.0	9.9	0.13	3.4%	67.9%	7730	65.1	299	32.5
C.1	132	7	20.3	9.8	0.13	3.4%	67.4%	4691	60.8	297	32.2
C.1	132	8	20.0	10.8	0.15	3.8%	68.6%	4134	61.4	298	33.5
C.1	132	8	19.9	10.6	0.15	3.7%	69.0%	3795	55.0	298	33.0
C.2	132	-	20.8	10.9	0.16	4.0%	69.5%	4764	39.6	299	29.1
C.2	132	-	20.6	10.7	0.15	3.9%	69.7%	4849	45.3	300	32.8
C.2	132	1 / 2 / 3	20.1	11.0	0.16	4.1%	72.9%	16096	49.1	299	29.3
C.2	132	1 / 2 / 3	20.0	10.9	0.16	4.1%	73.9%	32615	46.9	300	31.3
C.2	132	4	19.9	11.0	0.16	4.1%	73.8%	18511	57.0	300	29.0
C.2	132	4	20.5	10.7	0.16	4.0%	72.3%	5499	57.0	300	41.0
C.3	132	-	20.5	11.0	0.13	3.2%	57.1%	5180	2523.8	301	26.4
C.3	132	-	20.6	10.9	0.14	3.6%	63.5%	4894	1381.0	302	29.3
C.3	132	5	20.7	10.9	0.16	3.9%	69.9%	4981	40.2	304	28.5
C.3	132	5	-20.7	-10.9	0.14	3.6%	63.5%	4550	1250.0	302	29.3
C.3	132	6	20.5	10.9	0.16	4.0%	71.1%	5925	38.9	301	32.1
C.3	132	7	20.0	11.1	0.16	4.0%	71.6%	4327	48.8	299	28.0
C.3	132	7	20.0	11.0	0.16	4.0%	71.5%	4596	44.3	299	29.6
C.3	132	7	20.0	11.0	0.16	4.0%	71.3%	4948	53.8	299	32.3
C.3	132	7	20.3	10.8	0.16	4.0%	72.0%	7388	46.8	297	32.0
C.3	132	8	20.0	10.8	0.16	3.9%	71.7%	4313	52.5	298	31.4
C.3	132	8	20.0	10.7	0.15	3.9%	71.6%	4023	51.5	298	30.9
C.4	132	-	21.4	11.0	0.18	4.5%	74.4%	7973	40.3	297	33.6
C.4	132	-	21.5	10.9	0.18	4.5%	74.6%	8962	38.2	297	34.6
C.4	132	1	21.3	11.3	0.18	4.4%	73.4%	6952	37.7	302	26.9
C.4	132	1	21.3	11.2	0.18	4.4%	73.6%	9954	36.2	301	29.0
C.4	132	2	21.4	11.2	0.18	4.5%	73.5%	8060	363.6	298	28.2
C.4	132	2	21.4	11.2	0.18	4.4%	73.6%	11346	326.5	299	30.1
C.4	132	3	21.0	11.4	0.18	4.5%	74.0%	32579	49.0	300	26.4
C.4	132	3	21.1	11.3	0.18	4.4%	73.5%	49006	42.4	300	27.3
C.4	132	4	21.1	11.1	0.17	4.4%	73.7%	5805	40.4	300	34.0
C.4	132	4	21.6	10.9	0.17	4.3%	72.0%	5037	42.7	300	40.4

Manufacturer 3 / Sample C

No.	Area	Cycle No.	Isc	Uoc	Pmax	Eff.	FF	Rp	Rs	G	Tamb
	cm2		mA	V	W	%	%	Ohm	Ohm	W/m2	°C
C.8	132	5	20.5	9.5	0.13	3.3%	65.6%	6082	56.9	290	34.7
C.8	132	5	20.5	9.5	0.13	3.4%	66.4%	5485	56.9	291	34.0
C.15	132	-	21.6	10.6	0.16	4.0%	69.3%	3882	41.4	300	38.3
C.15	132	-	21.6	10.6	0.16	4.1%	69.7%	3867	43.4	293	38.9
C.15	132	8	20.5	10.9	0.16	4.0%	71.2%	6663	48.8	299	32.3
C.15	132	8	20.5	10.8	0.16	4.1%	72.5%	6224	45.8	298	32.1
C.15	132	8	20.5	10.7	0.16	4.0%	71.2%	6011	47.5	299	32.5
C.15	132	9	20.5	10.8	0.16	4.0%	73.0%	5146	48.5	304	14.1

C.15	132	9	20.5	10.7	0.16	4.0%	72.7%	4827	47.5	303	18.9
C.15	132	10	20.5	10.7	0.16	4.0%	73.8%	4572	55.3	304	18.3
C.15	132	11	20.0	10.8	0.16	4.1%	74.2%	5439	53.2	295	30.9
C.15	132	11	20.0	10.6	0.16	4.1%	74.5%	6537	47.5	295	30.0
C.15	132	11	20.0	10.6	0.16	4.1%	74.8%	7052	57.0	294	30.4
C.15	132	12	20.0	10.7	0.16	4.1%	74.0%	5184	53.2	292	28.8
C.15	132	12	20.3	10.5	0.16	4.1%	73.9%	7990	53.2	292	31.2
C.15	132	13	20.0	10.6	0.16	4.1%	75.0%	7780	51.5	298	29.1
C.15	132	13	20.5	10.6	0.16	4.1%	72.9%	10390	49.4	297	29.2
C.15	132	14	20.5	10.6	0.16	4.0%	73.7%	5914	48.5	304	28.6
C.15	132	14	20.5	10.5	0.16	4.0%	73.8%	5996	52.2	303	30.6
C.18	132	-	21.8	10.7	0.17	4.3%	73.9%	6746	36.5	301	41.7
C.18	132	-	21.2	11.0	0.17	4.3%	72.9%	6457	42.7	298	31.3

Manufacturer 4 / Sample D

No.	Area	Cycle No.	Isc	Voc	Pmpp	FF	η	Rp	Rs	G	Tmpv
	cm2		mA	V	W	%	%	Ohm	Ohm	W/m2	°C
D.1	60	-	11.1	4.8	0.04	2.4%	82.1%	15131	20.5	301	31.8
D.1	60	-	11.2	4.7	0.04	2.4%	81.8%	7495	22.1	300	36.6
D.1	60	1	34.7	4.3	0.07	4.0%	47.7%	1039	51.7	302	32.7
D.1	60	1	34.9	4.2	0.08	4.2%	51.5%	1272	42.5	301	34.3
D.1	60	2	34.8	4.2	0.08	4.4%	55.0%	2157	34.6	299	31.8
D.1	60	2	34.9	4.1	0.08	4.5%	55.6%	2265	32.6	299	33.6
D.1	60	3	34.2	4.2	0.07	3.7%	46.8%	810	58.3	304	30.6
D.1	60	3	34.5	4.2	0.07	3.7%	46.2%	553	58.4	304	31.6
D.1	60	3	34.2	3.8	0.07	3.8%	52.0%	690	31.7	302	30.7
D.1	60	3	34.2	3.7	0.07	3.7%	52.5%	1152	37.0	300	33.7
D.1	60	4	33.2	4.2	0.05	2.6%	33.2%	359	96.8	299	6999.0
D.1	60	4	33.7	4.0	0.05	2.7%	36.8%	656	77.2	299	6999.0
D.2	60	-	34.0	4.3	0.07	3.9%	48.5%	1119	46.2	299	30.0
D.2	60	-	34.2	4.3	0.07	3.7%	45.3%	905	56.4	299	34.6
D.2	60	1	33.8	4.3	0.07	3.9%	48.5%	1057	45.9	302	26.7
D.2	60	1	33.9	4.3	0.07	3.9%	49.0%	1166	43.7	302	28.5
D.2	60	2	33.9	4.3	0.07	4.0%	49.2%	1823	47.6	299	27.5
D.2	60	2	34.1	4.2	0.07	3.9%	48.7%	1597	47.8	299	31.4
D.2	60	3	34.2	3.8	0.07	3.9%	55.2%	1091	27.5	303	34.8
D.2	60	3	34.2	3.8	0.07	3.9%	54.6%	682	26.6	303	36.5
D.2	60	3	33.2	3.8	0.07	3.9%	55.1%	2285	30.4	300	30.7
D.2	60	3	33.7	3.8	0.07	3.9%	55.1%	1801	30.6	298	33.0
D.2	60	3	33.6	3.9	0.06	3.4%	45.4%	893	51.7	296	36.6
D.2	60	4	23.7	3.8	0.06	3.6%	51.2%	1420	35.5	297	31.7
D.3	60	-	34.2	4.0	0.08	4.6%	61.7%	1563	18.6	301	28.3
D.3	60	-	34.3	3.9	0.08	4.7%	62.6%	1701	17.6	301	31.0
D.3	60	5 / 6	35.1	3.7	0.07	4.1%	56.1%	1258	15.7	300	43.0
D.3	60	7	21.6	2.0	0.01	0.5%	22.2%	74	113.5	300	6999.0
D.3	60	7	18.7	1.8	0.01	0.4%	22.0%	81	127.3	293	32.3
D.4	60	-	34.4	4.0	0.08	4.6%	59.3%	1510	20.1	301	28.2
D.4	60	-	34.5	4.1	0.08	4.2%	53.3%	1177	35.2	300	31.7
D.4	60	5	34.4	4.1	0.08	4.6%	60.0%	1633	15.6	301	26.6
D.4	60	6	34.5	3.9	0.07	4.1%	53.9%	1526	23.8	300	31.8
D.4	60	6	34.5	3.9	0.07	4.1%	54.1%	1564	23.5	299	32.3
D.4	60	7	15.8	2.3	0.01	0.4%	21.5%	142	170.1	298	33.0
D.4	60	7	15.7	2.2	0.01	0.4%	21.3%	101	179.8	298	35.6
D.5	60	-	35.8	3.8	0.08	4.2%	55.7%	1257	24.2	301	35.7

Manufacturer 5 / Sample I

	cm2		mA	V	W	%	%	Ohm	Ohm	W/m2	°C
I.1	36	-	17.3	4.1	0.04	3.4%	51.8%	1191	38.1	300	31.5
I.1	36	-	17.6	4.1	0.04	3.4%	51.7%	1081	51.0	300	34.5
I.2	36	-	18.4	4.2	0.04	3.9%	55.2%	1831	52.4	300	34.1
I.2	36	-	18.4	4.2	0.04	3.9%	54.4%	1787	54.6	300	34.4
I.2	**36**	**5**	13.0	4.2	0.01	1.2%	24.4%	333	268.3	300	31.8
I.2	**36**	**5**	12.9	4.0	0.01	1.2%	25.2%	336	305.1	299	34.8
I.2	**36**	**5**	12.9	4.1	0.01	1.2%	24.2%	310	304.8	299	36.3
I.2	36	3	3.2	4.2	0.00	0.4%	34.5%	546	193.5	300	6999.0
I.2	36	3	2.8	4.1	0.00	0.4%	38.1%	1175	199.2	298	6999.0
I.2	36	3	3.1	4.0	0.00	0.4%	32.3%	0	-32.3	297	41.7
I.2	36	4	1.6	4.0	0.00	0.1%	23.2%	607	1185.2	294	33.8
I.2	36	4	1.1	3.7	0.00	0.0%	8.3%	310	549.9	294	35.9
I.3	36	-	18.5	4.1	0.04	3.3%	46.2%	863	67.0	299	33.1
I.3	36	-	18.7	4.1	0.04	3.3%	46.2%	831	69.4	300	36.5
I.3	**36.0**	5	11.94	**4.1**	0.0126	**0.0**	0.2576	**371**	339.0	**300.6**	6999
I.3	**36.0**	5	11.89	**4.1**	0.0123	**0.0**	0.2553	**379**	337.2	**300.1**	6999
I.3	35	6	5.54	4.0	0.01	0.5%	25.2%	706	720.2	299	37.5
I.3	36	6	7.00	4.0	0.01	0.5%	25.2%	726	740.8	299	37.5
I.3	36	7	4.3	4.1	0.01	0.5%	29.7%	909	897.3	293	34.0
I.3	36	7	4.2	4.0	0.00	0.5%	29.5%	982	889.7	295	35.6

Manufacturer 5 / Sample J

	cm2		mA	V	W	%	%	Ohm	Ohm	W/m2	°C
J.4	86.4	-	16.6	8.9	0.08	3.2%	56.8%	3355	95.3	301	43.6
J.4	86.4	-	16.7	8.9	0.08	3.3%	57.2%	4422	90.8	301	45.4
J.5	86.4	-	17.5	8.7	0.09	3.5%	60.1%	3351	76.9	300	41.7
J.5	86.4	-	17.6	8.7	0.09	3.5%	59.8%	3731	78.4	300	45.9
J.5	86.4	1	17.4	8.6	0.08	3.2%	55.6%	2701	107.0	300	39.6
J.5	86.4	1	17.7	8.6	0.08	3.3%	55.8%	2557	97.2	301	42.9
J.5	86.4	6	17.9	8.8	0.09	3.4%	55.9%	2372	88.1	300	42.0
J.5	86.4	6	17.7	8.7	0.09	3.3%	56.3%	2373	79.4	301	44.3
J.5	86.4	6	17.7	8.7	0.09	3.4%	56.8%	2788	76.2	300	45.7
J.5	86.4	7	17.4	8.4	0.07	2.9%	50.7%	1329	114.0	296	39.4
J.5	86.4	7	17.4	8.4	0.07	2.9%	50.6%	1218	114.0	297	40.5
J.5	86.4	11	16.3	6.8	0.04	1.4%	32.0%	617	268.9	295	34.0
J.5	86.4	11	16.3	6.8	0.04	1.4%	32.1%	624	297.5	295	35.1
J.5	86.4	12	15.3	6.2	0.03	1.1%	29.6%	512	294.9	294	32.3

Manufacturer 5 / Sample J

	cm2		mA	V	W	%	%	Ohm	Ohm	W/m2	°C
J.3	86.4	-	17.5	8.6	0.09	3.4%	58.0%	3782	101.5	301	42.5
J.3	86.4	-	17.6	8.6	0.09	3.4%	58.1%	4464	95.4	300	40.7
J.3	86.4	1	17.2	8.5	0.08	3.0%	53.1%	2207	132.3	301	41.6
J.3	86.4	1	17.3	8.5	0.08	3.0%	52.8%	2341	135.4	300	43.6
J.3	86.4	6	17.4	8.6	0.08	3.0%	52.3%	2581	91.8	301	47.8
J.3	86.4	6	17.5	8.6	0.08	3.1%	52.9%	2173	117.3	301	49.0
J.3	86.4	7	16.8	8.5	0.07	2.8%	50.9%	6831	126.6	296	37.4
J.3	86.4	7	16.9	8.4	0.07	2.8%	50.8%	4863	138.4	297	39.0

J.3	86.4	7	16.3	7.8	0.06	2.4%	48.0%	2351	218.4	296	38.6
J.5	86.4	-	-16.9	8.8	0.09	3.5%	-59.7%	2139	75.9	296	37.6
J.5	86.4	-	16.9	8.8	0.09	3.4%	59.2%	3068	91.2	297	38.4
J.5	86.4	8	17.4	8.5	0.07	2.7%	47.7%	1351	142.5	299	40.1
J.5	86.4	8	17.4	8.5	0.07	2.7%	47.9%	1370	117.7	299	39.3
J.5	86.4	9	17.4	8.4	0.07	2.6%	48.3%	1114	130.2	307	5.1
J.5	86.4	9	17.4	8.4	0.07	2.6%	47.1%	1141	123.5	304	11.1
J.5	86.4	10	16.9	6.8	0.04	1.5%	32.9%	614	303.3	302	25.3
J.5	86.4	10	16.9	6.9	0.04	1.5%	33.0%	630	291.7	301	26.5
J.6	86.4	-	16.3	9.1	0.09	3.4%	59.5%	2428	100.4	299	39.2
J.6	86.4	-	16.3	9.1	0.09	3.4%	58.8%	2598	100.4	298	39.9
J.6	86.4	8	16.9	8.7	0.07	2.6%	47.3%	1430	180.4	306	28.8
J.6	86.4	8	16.9	8.7	0.07	2.6%	46.7%	1446	151.9	304	33.3
J.7	86.4	-	17.6	8.7	0.08	3.2%	54.3%	2435	95.4	300	46.9
J.7	86.4	-	17.6	8.6	0.08	3.2%	54.4%	2368	95.4	299	48.5
J.7	86.4	2	17.5	8.6	0.08	3.2%	54.4%	2325	74.1	299	37.2
J.7	86.4	2	17.6	8.6	0.08	3.1%	53.9%	2301	81.5	300	42.1
J.7	86.4	3	17.4	8.8	0.08	3.3%	55.0%	2164	111.8	299	3521.4
J.7	86.4	3	17.4	8.8	0.08	3.2%	54.6%	2130	123.5	298	742.1
J.7	86.4	4	16.8	8.7	0.08	3.2%	55.2%	4073	133.0	296	32.7
J.7	86.4	4	16.9	8.8	0.08	3.1%	53.9%	3483	137.7	297	33.7
J.7	86.4	8	17.4	8.3	0.07	2.6%	46.5%	1393	139.2	299	38.7
J.7	86.4	8	17.4	8.3	0.07	2.6%	47.0%	1388	95.0	303	39.1
J.8	86.4	-	17.5	8.6	0.09	3.3%	57.2%	3394	96.3	299	43.0
J.8	86.4	-	17.5	8.7	0.09	3.3%	57.0%	2965	98.1	299	44.7
J.8	86.4	5	17.6	8.9	0.08	3.2%	53.5%	2976	1163.5	300	38.8
J.8	86.4	5	17.5	8.8	0.09	3.4%	56.4%	2527	196.3	300	43.0
J.8	86.4	3	16.9	9.0	0.08	3.2%	54.4%	3007	107.2	299	41.8
J.8	86.4	3	16.9	8.9	0.08	3.2%	55.5%	3810	121.6	301	45.2
J.8	86.4	3	16.9	9.0	0.08	3.2%	54.6%	2856	123.4	300	47.5
J.8	86.4	3	16.9	8.9	0.08	3.2%	54.6%	10333	109.2	300	48.9
J.8	86.4	4	16.9	9.0	0.08	3.2%	54.2%	3949	109.2	298	36.1
J.8	86.4	4	16.9	8.9	0.08	3.2%	54.6%	3883	109.2	298	37.2
J.8	86.4	8	16.9	8.5	0.07	2.7%	49.1%	1729	142.5	302	35.0
J.8	86.4	8	17.4	8.5	0.07	2.7%	48.3%	1719	133.0	304	37.8
J.10	86.4	-	17.4	8.7	0.09	3.3%	56.3%	2955	94.9	296	31.8
J.10	86.4	13	17.3	8.6	0.08	3.0%	51.2%	2030	124.5	298	30.6
J.10	86.4	13	17.4	8.6	0.08	3.0%	51.3%	2072	129.1	298	31.9
J.10	86.4	14	17.4	8.7	0.08	3.0%	50.6%	2079	135.3	301	32.0
J.10	86.4	14	17.4	8.7	0.08	3.0%	51.1%	2063	130.6	301	30.1

Manufacturer 6 / Sample K

	cm2		mA	V	W	%	%	Ohm	Ohm	W/m2	°C
K.1	797	6	689.1	2.0	0.98	4.1%	71.7%	12704	0.00	301	31.3
K.1	797	6	694.8	1.9	0.97	4.1%	72.2%	12704	0.00	301	36.2
K.1	797	7	733.3	2.0	1.04	4.4%	72.3%	119	0.43	297	32.9
K.1	797	7	734.0	2.0	1.04	4.4%	72.4%	103	0.43	297	32.2
K.2	797	-	742.8	1.9	1.04	4.3%	72.5%			302	33.9
K.2	797	-	742.0	1.9	1.04	4.3%	72.3%			303	34.4
K.3	797	3	731.0	2.0	1.01	4.2%	70.4%			301	34.5
K.3	797	3	729.3	2.0	1.02	4.2%	70.9%			302	33.4
K.3	797	4	683.3	2.0	0.97	4.1%	72.4%	156	0.54	296	32.3
K.3	797	4	686.0	1.9	0.97	4.1%	72.7%	135	0.47	297	33.5

9. LITERATURE

[1] "New generation of solar hybrid collectors / Phase 1", P. Affolter (LESO/EPFL), D. Ruoss, P. Toggweiler (Enecolo AG), A. Haller (Schweizer AG), OFEN Project No 56360/1686, November 1997

[2] "Long Term Behaviour of Passively Heated or Cooled a-Si:H modules", C. Hof, M. Lüdi, M. Goetz, D. Fischer, A. Shah, Institute of Microtechnology, Université of Neuchâtel, 25th IEEE PVSC, Washington DC, May 13-17, 1996

[3] « Grenzbelastbarkeit von PV-Modulen», Hermann Laukamp and al., Fraunhofer-Institut für Solare Energiesysteme ISE, OTTI Symposium PV Solarenergie, 10-12 März 1999

[4] « Belastbarkeitsgrenzen von PV-Modulen», Verbundprojekt: Qualifizierung von PV-Fassadenelementen, Hermann Laukamp and al., Fraunhofer-Institut für Solare Energiesysteme ISE, Freiburg im Breisgau, April 1998

[5] « Interface Degradation in a-Si:H Solar Modules», D. Peros and al., Universität-GH Siegen, Institut für Halbleiterelektronik, 14th European Photovoltaic Solar Energy Conference and Exhibition, Barcelona (Spain), 30.6 – 14.7 1997

[6] "Solarzellen aus amorphem Silizium auf Aluminium: drei Wege, den Substrateinfluss zu beschreiben", M. Götz, Thèse No 1637, Dép. Microtechnique. EPFL, 1997